Scuola Internazionale Superiore Studi Avanzati-S.I.S.S.A
International School for Advanced Studies -I.S.A.S

Trieste, Italy

Calcium-activated chloride channels in mouse vomeronasal sensory neurons

Thesis submitted for the degree of *"Doctor Philosophiae"*

Academic year 2012/13

CANDIDATE

Asma Amjad

SUPERVISOR

Prof. Anna Menini

To my loving parents…

Declaration

The work included in this thesis has been carried out at International School for Advanced Studies, Trieste, between November 2009 and September 2013.

This work is included in:

1. Dibattista M, **Amjad A**, Maurya DK, Sagheddu C, Montani G, Tirindelli R, Menini A (2012) Calcium-activated chloride channels in the apical region of mouse vomeronasal sensory neurons.
   J Gen Physiol. 2012 Jul 140(1):3-15

2. **Amjad A,** Pifferi S, Boccaccio A, Menini A. Characterization of Ca^{2+}-activated chloride current in isolated mouse vomeronasal sensory neurons
   Manuscript in preparation

The data reported here is an outcome of the experiments performed by me and, for the published article Dibattista *et al*. 2012, some electrophysiological experiments were performed in collaboration with Michele Dibattista and Claudia Sagheddu and immunocytochemistry on isolated neurons performed in collaboration with Devendra K. Maurya.

Abstract

In vomeronasal sensory neurons, signal transduction occurs in microvilli that are present at the neuron's apical surface. The binding of pheromone to vomeronasal receptors causes an increase of the intracellular calcium concentration by calcium entry through TRPC2. An important issue is the impact of Ca^{2+} entry in pheromonal transduction.

In the first part of this thesis we have investigated the functional role played by the increase in intracellular Ca^{2+} concentration in the apical region of vomeronasal sensory neurons. By taking advantage of flash photolysis of caged calcium restricted to the apical region of neurons, we have measured a calcium-activated current with the whole-cell voltage-clamp technique. Our results demonstrated that a large current is indeed activated by calcium in the apical region of mouse vomeronasal sensory neurons and our immunohistochemistry data has revealed the presence of the proteins TMEM16A and TMEM16B, responsible for calcium-activated chloride channels, in the microvilli of vomeronasal sensory neurons. Therefore we have concluded that calcium-activated chloride channels are present at high density in the region where signal transduction occurs and therefore may play an important role in vomeronasal transduction.

In the second part of this thesis we have characterized in more detail the calcium activated currents in mouse vomeronasal sensory neurons using the whole-cell voltage-clamp technique in the presence of various intracellular Ca^{2+} concentrations. From the dose-response relation we determined that the Ca^{2+} concentration necessary to activate 50% of the maximal current was 1.4 µM at -100 mV and 0.6 µM at +100 mV. From ion selectivity experiments, we found that the current is carried by anions. Moreover, we demonstrated that some of the commonly used Cl^- channel blockers, NFA and $CaCC_{inh\text{-}A01}$, do inhibit the Ca^{2+}-activated current in vomeronasal sensory neurons. Further studies with knockout mice for TMEM16A or TMEM16B will be necessary to establish the physiological role of these channels in vomeronasal transduction.

Table of Contents

Introduction

1.1 Pheromones.

From the refreshing fragrance of a lover's perfume to the strong aroma of *illy's* "cappuccino", our sense of smell is responsible for the recognition of familiar odors. Animal constantly inspect their external environment not only for food sources but also for social interactions and reproductive behavior. Our chemical way to communicate among the species is the release and the detection of special substances in the external environment, which are responsible for an extensive range of social behaviors such as finding a mate, regulating the level of aggression, communal supremacy and mediating the recognition of kin and non-kin. The substances which convey a chemical message among animals are termed as *"Semio-chemicals*" from the Greek "semion" (sign). An important class of *semio-chemicals* is constituted by *Pheromones*. The term pheromone was first introduced in 1959 by the entomologists Peter Karlson and Martin Luscher (Karlson & Luscher, 1959) and is based on the two Greek words "*pherein*" (to transport/transfer) and "hormon" (to stimulate). They defined pheromones as *"substances secreted to the outside by an individual and received by a second individual of the same species, in which they release a specific reaction, for example, a definite behavior or developmental process*." The term pheromone is strictly reserved for the chemical signals that are produced and received by the members of the same species (Wyatt, 2003).

Subject to the final outcome, these chemical signals can be categorized accordingly. They can vary from releaser pheromone that elicit a specific and immediate behavioral effect, to primer pheromones which elicit a long term effect on endocrine state and development. In the same year, when Karlson and Luscher defined the term pheromone, the first insect pheromone, bombykol, was identified (Butenandt *et al*., 1959). Afterwards, pheromones have been identified also in mammals. One of the most amazing example is the discovery of a small volatile molecule (Z)-7-dodecen-1-yl acetate that is a sex pheromone and is released in the urine of female Asian elephant and is also present in around 140 species of moth as

a component of their female sex pheromone. The use of a single compound as a signal by different species, illustrate a common phenomenon of independent evolution of particular molecules (Kelly, 1996).

A wide variety of chemicals are used as pheromones which include small volatile molecules, proteins and peptides. In a chemosensory system specialized for detecting chemical cues at a distance, some properties are important which will determine the efficacy of pheromone. In terrestrial vertebrates one must expect that the volatility is one of the features of released chemicals. But most of the biological sources of these signals contain water and lipids and they should pass through fluid covering sensory epithelium before they transduce the sensory signal. For example attractant and alarm pheromone need to be small and volatile, such as male mouse urinary constituent (methylthio) methanethiol (MTMT), which attracts female investigation (Lin *et al*., 2005). Their small size and volatility not only ensures that such pheromones are dispersed rapidly, but also makes these signals transient. In contrast, pheromonal signals that need to be associated with a specific individual or place in the environment are ideally nonvolatile, so that they do not disperse and are longer lasting. For example, male mice deposit urine marks containing 18–20 kDa major urinary proteins (MUPs), the stability and in volatility of which make them ideal for their territorial marking role (Hurst & Beynon, 2004).

Animals use a number of mechanisms for releasing pheromones in the external environment. In some cases, like in rodents, these cues are excreted intentionally in feces or in urine to be used as a territorial markers. These cues are comprised of a mixture of small volatile molecules along with sulfated steroids and proteins having pheromonal functions (Novotny, 2003; Nodari *et al*., 2008; Chamero *et al*., 2007). A number of chemosignals have been identified also in the saliva of different species for example sexual pheromones of boars (Loebel *et al*., 2000). Some pheromones are secreted in the vaginal secretions, for example hamsters release aphrodisin, a sexual attractant pheromone (Mägert *et al*., 1999).

1.2 Pheromone Detection Systems

The species specificity of pheromones conveyed a high rate of evolutionary alterations of the chemosensory systems responsible for their detection. Chemical senses are the oldest senses and are shared by all organisms including bacteria, so animals are pre-adapted to detect chemical signals in the environment (Wilson, 1970). With the transition from aquatic to terrestrial environment, evolution brought the possibility to detect large airborne chemosignals by the ciliated cells of what came to be main olfactory systems. However, sensitivity to water soluble but relatively in-volatile chemosignals of the aquatic environment was not lost. Instead, the microvillar cells of the ancestral olfactory organ became largely segregated in an anatomically separate organ, in early terrestrial vertebrates, known as the vomeronasal organ (VNO), at the same time that the main olfactory system was adapting to sense airborne volatile stimuli. However, the detailed picture is considerably more complicated (Eisthen, 2004). Although most of the olfactory sensory neurons are ciliated and express olfactory receptors, there are also microvillar cells that appear to form a distinct chemosensory system (Elsaesser *et al*., 2005).

For many years the standard view of pheromone sensing was based on the assumption that the vomeronasal and the main olfactory systems have separate functions. However, there are evidences indicating that some behaviors are mediated exclusively by one or by a complementary action of both systems. For example (Bruce, 1959) reported that, when female mice that have been recently inseminated are exposed to urine of a male different from the one they mated with, the pregnancy is interrupted and the female returns to estrus. This effect depends on a functional vomeronasal system (Bellringer *et al*., 1980). Differently, the nipple search in rabbit pups is one of the typical examples of behavior strictly dependent on an intact main olfactory system (Hudson & Distel, 1986). In other instances, behavioral responses are mediated by both the vomeronasal and the main olfactory systems. This is the case of female hamsters, whose ultrasonic calling during estrus is abolished by the inactivation of either the vomeronasal or the main olfactory system (Johnston, 1992). Therefore, the simple story of two distinct chemosensory

systems with separate functions is in reality more complicated with a complex interplay between them. Moreover, other subsystems such as the septal organ of Masera and the Grüneberg ganglion may also play a role in pheromone detection. In the following sections, I will first briefly describe the chemosensory systems involved in the pheromone detection and then I will more extensively describe the vomeronasal system, which is the subject of the present thesis work.

1.2.1 Main Olfactory System

In vertebrates, the main olfactory epithelium is a pseudo-stratified epithelium composed of three type of cells: olfactory sensory neurons, supporting cells and basal cells. The olfactory sensory neurons are bipolar neurons with a single ciliated dendrite extending to the mucosal surface. These cilia are the site of olfactory transduction. Axons project in the distinct domain of main olfactory bulb. Most OSNs express only 1 of 1,000 odorant receptor genes (Buck & Axel, 1991; Zhang *et al*., 2004)

In the main olfactory bulb, glomeruli are quite well anatomically separated, surrounded by periglomerular cells, and rather uniform in size (about 50μm diameter in mice). Axons of all the olfactory sensory neurons expressing a particular odorant receptor converge to only two glomeruli in the main olfactory bulb (Ressler *et al*., 1993; Vassar *et al*., 1993; Mombaerts *et al*., 1996). In mice there are about 2,000 glomeruli, and their localization is roughly conserved among individuals. Therefore the olfactory bulb is topographically organized, with each glomerulus representing a single type of odorant receptor. In the main olfactory bulb, a single mitral cell with its dendritic arborizations makes synapses at the level of only one glomerulus. The axons of mitral and tufted cells project through the lateral olfactory tract to the olfactory cortex.

1.2.2 Septal Organ of Masera

The septal organ, or organ of Masera, is a small island of neuroepithelium lying in the ventral base of nasal septum near the entrance of the nasopharynx. This chemosensory system has been observed in many mammals including rat, mouse, guinea pig, hamster etc. (Rodolfo-Masera, 1943; Adams & McFarland, 1971;

Bojsen-Moller, 1975; Katz & Merzel, 1977; Breipohl *et al*., 1983; Breipohl *et al*., 1989). The cellular organization of the septal organ resembles that of the main olfactory epithelium and it is composed of bipolar olfactory sensory neurons with cilia, supporting cells and Bowman's glands. Neurons project their axons in the posterior ventromedial olfactory bulb.

These neurons are extremely sensitive to some odorants with a nanomolar threshold (Grosmaitre *et al*., 2007). This is consistent with a previous electro-olfactogram study where septal organ responded to many chemicals with a lower threshold than the main olfactory epithelium (Marshall & Maruniak, 1986). The position of the septal organ in the nasal cavity suggests that the organ may function in the early detection of biologically relevant molecule, as those for example resulting from licking behavior.

1.2.3 Grüneberg Ganglion

Grüneberg discovered a ganglion of unknown function while examining nasal glands (Grüneberg, 1973). The Grüneberg ganglion (GG) is located in the interior vestibule of the nasal cavity. Unlike other chemosensory systems, it is composed of clusters of about 500 neurons (Grüneberg, 1973). These neurons were originally considered as a part of *nervus terminalis* but the absence of luteinizing hormone-releasing hormone dissolved this theory (Fleischer *et al*., 2006).

This organ is found in all mammals including humans. Only two types of cells have been identified in the GG which include glial cells and ciliated neurons (Brechbühl *et al.*, 2008). GG neurons express the olfactory marker protein and project to glomeruli in defined areas in the olfactory bulb suggesting a role for GG in chemosensory detection (Koos & Fraser, 2005; Fuss *et al*., 2005). Till date, the stimuli for these neurons are unclear. Since GG axon project to "necklace glomeruli" in the olfactory bulb, which are active during the suckling of pups, it was suggested that the GG may sense maternal pheromones (Fuss *et al*., 2005; Koos & Fraser, 2005; Roppolo D, 2006). Moreover a subpopulation of GG neurons responds to "alarm pheromones", volatile compounds released by the animals

subjected to stress to alert conspecifics about danger (Brechbühl *et al*., 2008; Brechbühl *et al*., 2013).

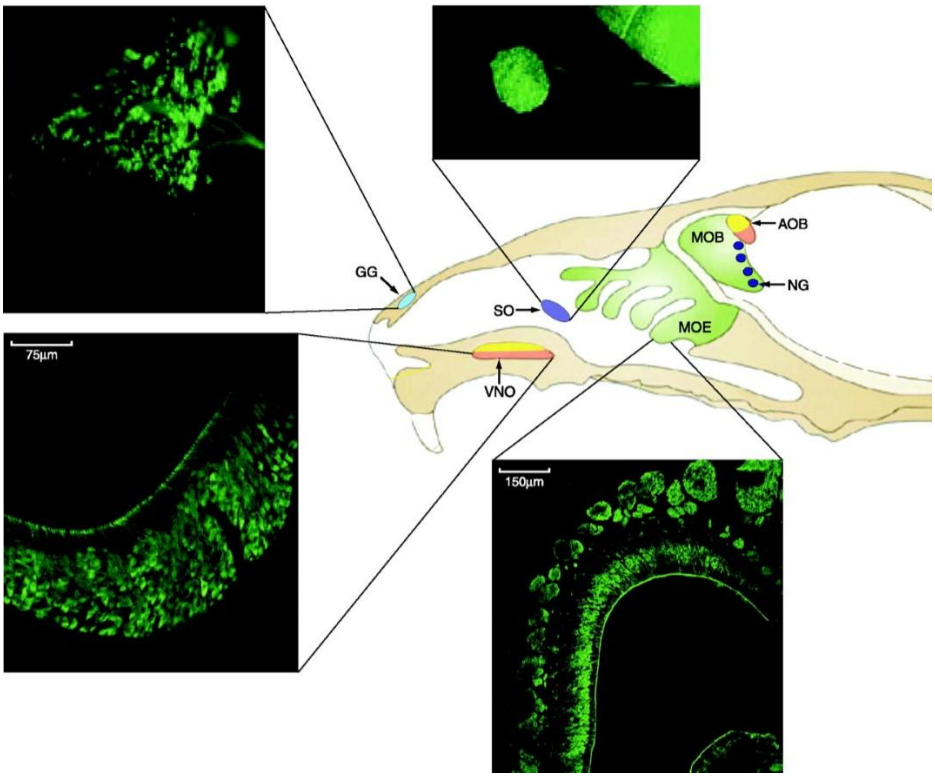

Fig1.1. Chemosensory systems in rodents. A simplified sagittal section of a rodent head showing the location of sensory epithelia: the main olfactory epithelium (MOE), the vomeronasal organ (VNO), the septal organ of Masera (SO), the Grüneberg ganglion (GG), and the location of the main olfactory bulb (MOB) with necklace glomeruli (NG) and of the accessory olfactory bulb (AOB) (modified from Mombaerts 2004). Insets show images obtained from the intrinsic green-fluorescent protein (GFP) fluorescence from olfactory marker protein (OMP)-GFP gene-targeted mice. Top left panel: the Grüneberg ganglion has an arrow-like shape with neurons clustered in small groups. Axons fasciculate and form a single nerve bundle (modified from Fuss *et al*. 2005). Top right panel: the septal organ of Masera is an island of sensory epithelium. Axons from sensory neurons form two bundles (modified from Levai and Strotmann *et al* 2003). Bottom left panel: mature vomeronasal sensory neurons in a coronal section of the vomeronasal organ. Bottom right panel: mature olfactory sensory neurons in a coronal section of the main olfactory epithelium (Tirindelli *et al*., 2009).

1.2.4 Vomeronasal System

In 1813 the Danish anatomist Ludwig Jacobson labeled an organ in the nose of mammals that had not been observed previously. He observed many glands in the organ with a rich supply of blood and presumed the secretory nature of the organ but supposed it as a sensory organ. This sensory organ is now known as Vomeronasal organ (VNO) of Jacobson. The vomeronasal organ is a tubular structure encased in a bony cartilaginous capsule located at the base of nasal septum (Døving & Trotier, 1998). In some amphibians and reptiles the sensory epithelium is freely exposed to the nasal airflow while in snakes and in some lizards it is sequestered in a separate cavity which opens into the mouth. Based on anatomical, electrophysiological and behavioral evidences it has been suggested that, in these animals, the chemical cues are delivered to the vomeronasal organ by the tongue (Meredith & Burghardt, 1978; Kubie & Halpern, 1976). In mammals, the VNO is sequestered in a separate cavity which may open in the nasal chamber or in the nasopalatine canal which connects nose and mouth (McCotter, 1912; Estes, 1972). The sensory vomeronasal epithelium, containing the vomeronasal sensory neurons, is found on the medial side of the vomeronasal organ. Given its sunken nature, the vomeronasal epithelium cannot be reached by the airstream that regularly flows through the nasal cavity. Thus, to provoke chemosensory response, molecules must dissolve in the nasal mucus and enter into the lumen. Lateral to the lumen are the blood vessels and sinuses that are innervated by the autonomic nervous system, which induces vasodilation and vasoconstriction thereby producing a pump-like action for stimulus access to the lumen. During sociosexual interaction, many mammals display a “flehmen behavior” in which they lift their head after contact with the odorant source, wrinkle their nose, lift their upper lip and stop breathing. In ungulates, the “flehmen behavior” is evoked by olfactory investigation of urine and vaginal secretions (Døving & Trotier, 1998). After exposure to pheromonal cues, norepinephrine accumulation has been measured in the vomeronasal organ. It is possible that hormonal release plays some role in the alteration of vascular tonicity and glandular secretion thus in turn increasing the receptivity of epithelium.

Therefore, the functioning of the vomeronasal organ is not a passive event but it can be modulated actively.

The medial concave side of the vomeronasal lumen is lined by a pseudo-stratified epithelium composed of three types of cells, sensory neurons, supporting cells and basal cells. The basal stem cells are embedded in the basal membrane of sensory and non-sensory epithelium (Giacobini *et al*., 2000). Supporting cells are found in the uppermost superficial layer. Vomeronasal sensory neurons are bipolar neurons. On their apical side they give rise to a long dendrite. At the tip of the dendrite is the terminal knob from where a number of microvilli protrude. Vomeronasal sensory neurons form two overlapping neuronal populations apical and basal, expressing members of V1R and V2R receptor family respectively. A long axon emerges from the basal side of the cell body and terminates in the accessory olfactory bulb.

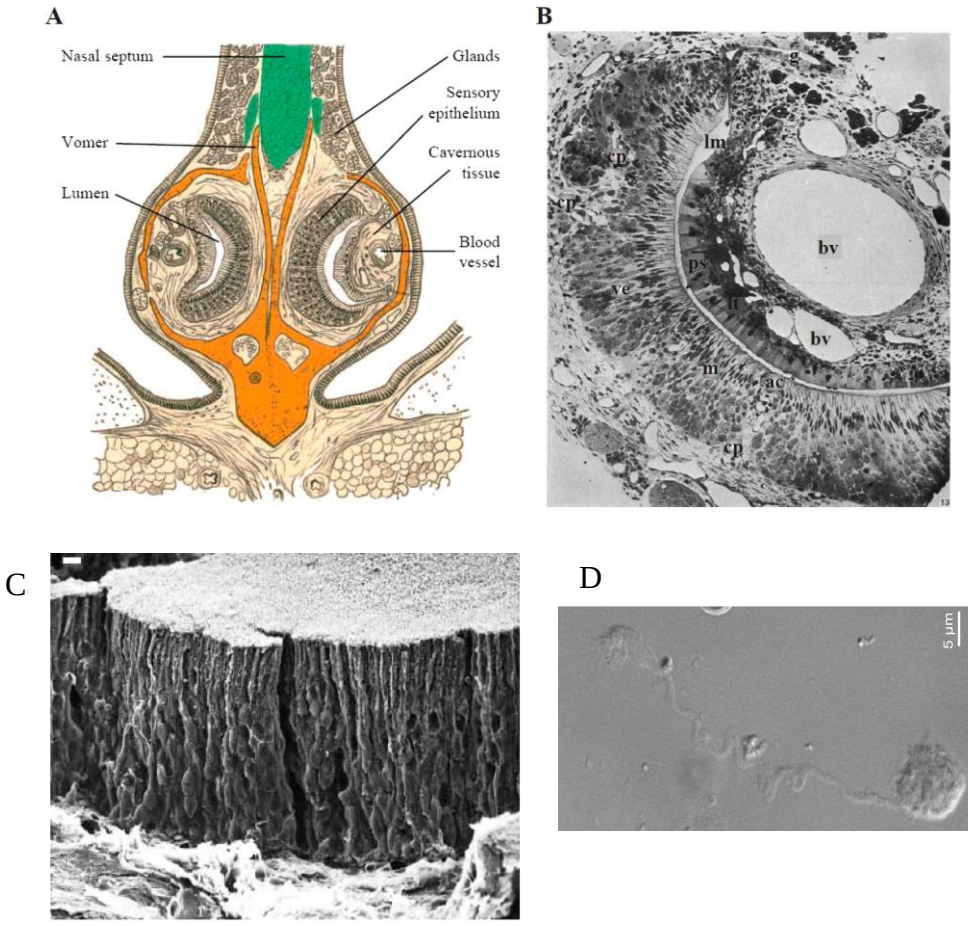

Fig 1.2: (A) A schematic cross section through the VNO. The bilateral organization is clearly visible as well as some of the substructure inside the VNO. Pheromones enter the luminal space and bind to VSN receptors located in the sensory epithelium. The blood vessel's pumping action facilitates pheromone exposure by constantly refreshing the luminal space. The general structure of the VNO is supported and protected by the vomer bone and cartilaginous tissue. (Adapted from Døving & Trotier, 1998). (**B)** Coronal section of the VNO at the central part of its middle segment. The vomeronasal epithelium (ve) covers all the medial wall (m) of the tube and a pseudostratified epithelium (ps) the lateral wall (lt). The organ shows its typical crescent shape. Blood vessels (bv) are located in the groove of the lateral external wall of the organ. A vomeronasal gland (g) opens at the superior edge of the lumen (lm). An area devoid of cellular processes (ac) overlying an intraepithelial (cp) capillary is seen. From (Vaccarezza *et al.*, 1981). (**C)** Scanning electron microscopy of an enlarged portion of rat vomeronasal sensory epithelium showed the packed VSNs. Scale bar 20 µm. (Reprinted from Trotier *et al*. 1998). (**D)** A confocal image of an isolated mouse VSN (scale 5µm)

VSNs project their axons to the accessory olfactory bulb where they synapse with the mitral cell projections in the glomerular structure. The neurons expressing V1R and V2R are segregated to the anterior and posterior part of the bulb respectively (Halpern & Martínez-Marcos, 2003). A subpopulation of V2R neurons that detect class one Major Histocompatibility Complex (MHC) molecule project axons to the posterior subdomain of the posterior subdivision of the bulb (Ishii *et al*., 2003). Genetically modified mice in which V1R expressing neurons have been labelled with different fluorescent markers reveal that mitral cells in the accessory olfactory bulb send a branched primary dendritic tree to sample information to glomeruli that receive information from another but closely related V1R receptor (Wagner *et al*., 2006). These findings gives the foundation that integration of information already begins at the level of the accessory olfactory bulb (Wagner *et al*., 2006).

Mitral cells of the accessory olfactory bulb project to areas of the limbic system, the medial amygdala and the posteromedial cortical amygdala (also called "vomeronasal amygdala"), the accessory olfactory tract, and the bed nucleus of the stria terminalis (Campenhausen & Mori, 2000).

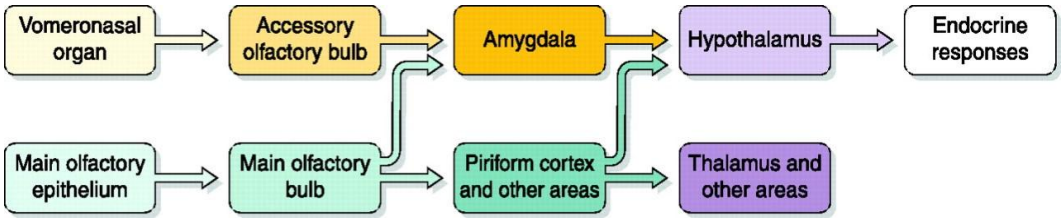

Fig 1.3: A schematic diagram showing the anatomical pathways of the rodent vomeronasal and main olfactory systems *(*Tirindelli *et al.,* 2009*).*

1.2.4.1 Vomeronasal Sensory Neurons and Signal Transduction

The detailed signal transduction cascade in VSNs is still largely unknown, although it is known that the stimuli produce membrane depolarization, intracellular Ca^{2+} increase, and increase in action potential firing rate (Boschat *et al*., 2002; Cinelli *et al*., 2002; Del Punta *et al*., 2002; Døving & Trotier, 1998; Holy *et al*., 2000; Inamura & Kashiwayanagi, 2000; Inamura *et al*., 1997; Leinders-Zufall *et al*., 2004; Leinders-Zufall *et al*., 2000; Lucas *et al*., 2003; Spehr *et al*., 2009; Stern & McClintock, 1998)

The vomeronasal epithelium has two subset of neurons, apical and basal. Apical neurons express members of vomeronasal receptor type 1(V1R) together with $G_{\alpha i2}$, whereas basal neurons express members of vomeronasal receptor type 2 (V2R) and $G_{\alpha o}$ (Dulac & Axel, 1995; Pantages & Dulac, 2000; Tirindelli *et al*., 2009)

V1R was the first family of vomeronasal receptors to be isolated (Dulac & Axel, 1995). A family of around 30 coding sequences for putative receptor proteins (V1Rs) expressed in VSNs was first cloned. Sequence analysis of these genes indicated that they constitute a separate family of protein having seven transmembrane domains that are unrelated to the receptors expressed in the olfactory epithelium (Buck & Axel, 1991). Latest genome analysis of mouse genome has revealed about 200 functional genes for V1R which are expressed by the VSNs present in the apical surface of the vomeronasal epithelium and express $G_{\alpha i2}$. They project their axon to the rostral part of the olfactory bulb (Wendy *et al*., 2005).

A second family of vomeronasal receptors, V2Rs, was discovered in 1997 (Ryba & Tirindelli, 1997; Matsunami & Buck, 1997; Herrada & Dulac, 1997) and in the mouse it accounts for about 120 potentially functional members. V2Rs are expressed by the VSNs that are present on the basal portion of vomeronasal epithelium which express Gαo subunit and projects their axon to the caudal part of olfactory bulb.

Moreover, a group of receptors belonging to the family of formyl peptide receptor has been found in the VNO (Rivière *et al*., 2009 ; Liberles *et al*., 2004) Formyl

peptide receptors are a seven membrane domain G-protein coupled receptors which are known to play a role in antibacterial host defense and inflammation (Migeotte *et al*., 2006; Ye *et al*., 2009). They are expressed mainly in mammalian phagocytic leukocyte and also show affinity for chemo attractants.

VSNs are highly sensitive to the detection of pheromones. For example The V1R expressing neurons respond to urinary volatile compounds, such as (R,R)-3,4-dehydro-exo-brevicomin (DB) and (S)-2-sec-butyl-4,5-dihydrothiazole (SBT), with thresholds of 10^{-10} to 10^{-11} M (Leinders-Zufall *et al*., 2000). Moreover V2R expressing neurons respond to MHC peptides at lower concentration up to 10^{-13}M (Leinders-Zufall *et al*., 2004).

The activation of receptors causes the release of βγ complex of the heteromeric G-proteins, Gαo and $G_{\alpha i2}$, which in turn activate phospholipase C (PLC). PLC hydrolyses phosphatidyl inositol biphosphate (PIP_2) into inositol 1, 4, 5 triphosphate (IP_3) and diacyl glycerol (DAG). The main target of PLC activation is the transient receptor potential canonical 2 (TRPC2). The expression of TRPC2 channel transcript in rat VSNs was shown through *in-situ* hybridization, where rTRPC2 antisense probe RNA marked both apical and basal neurons. Immune labelled images have shown the restricted expression of TRPC2 in the microvilli of VSNs (Liman *et al*., 1999). In another study it was revealed that TRPC2 are present along with G-protein subunits (Menco *et al*., 2001). TRPC2 knockout mice have confirmed the TRPC2 channel as a transduction channel. TRPC2 knockout mice were unable to discriminate between the sexes and also lost the male-male aggression specific behavior mediated by VNO (Leypold *et al*., 2002; Stowers *et al*., 2002). However, the basal neurons in mutant mice still showed the response to MHC peptides and TRPC2 knockout mice exhibited the Bruce effect (Kelliher *et al*., 2006).

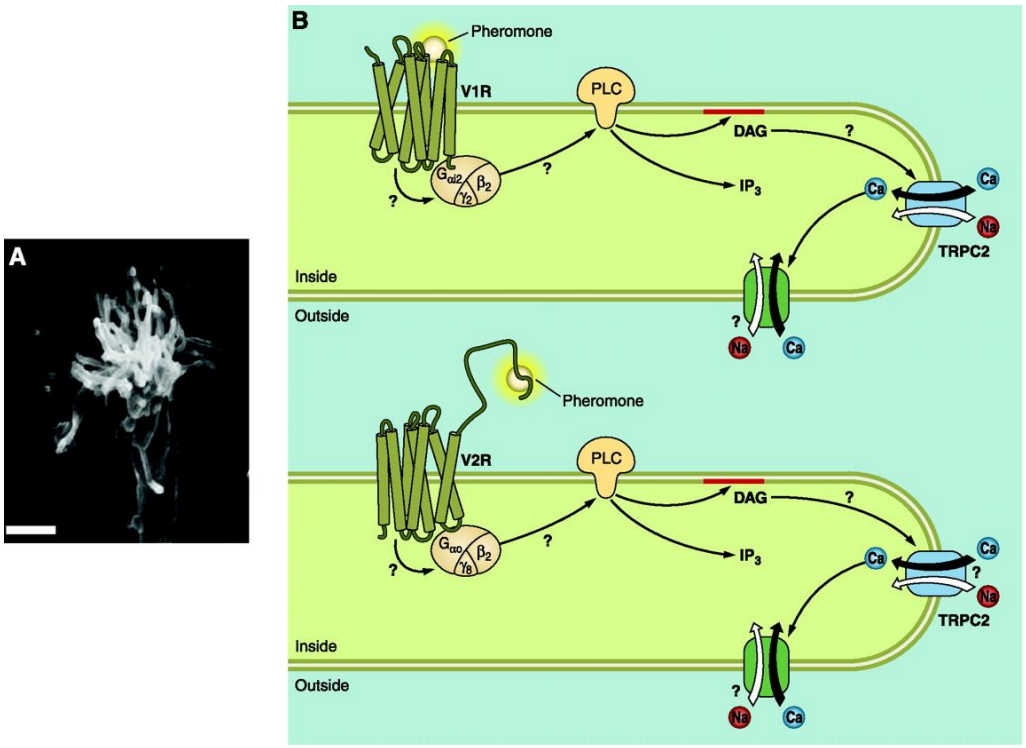

Fig 1.4: Transduction mechanisms in VSNs, **(A)** A scanning electron micrograph of the knob of a rat VSN showing several microvilli (Scale bar 1 μm) **(B)** Binding of pheromone molecules to vomeronasal receptors in the microvilli activates a transduction cascade involving V1R, $G_{\alpha i2\beta2\gamma2}$ in apical neurons, or V2R, $G_{\alpha o\beta2\gamma8}$ in basal neurons. The βγ complex activates the PLC that in turn may cause an elevation of IP3 and/or DAG. The gating of the TRPC2 channel allows an influx of Na^+ and Ca^{2+} ions causing a membrane depolarization. An additional cation-selective channel activated by Ca^{2+} may be involved in the transduction cascade. The TRPC2 channel appears to be the principal transduction channel in V1R-expressing neurons, whereas its role in V2R-expressing neurons in unclear *(*Tirindelli *et al.*, 2009*)*.

The TRPC2 channel is a Ca^{2+} permeable cationic channel. Its proposed mechanism of activation is similar to the signal transduction cascade in Drosophila phototransduction (Minke & Cook, 2002). Binding of pheromone to vomeronasal receptors causes the activation of G-proteins that in turn stimulate phospholipase C (PLC) and the production of lipid messenger diacylglycerol (DAG) (Lucas *et al*., 2003) and possibly other polyunsaturated fatty acid like arachidonic acid (Spehr *et al*., 2002; Zhang *et al*., 2008) and linoleic acid (Spehr *et al*., 2002).

The hydrolysis of PIP2 by PLC also leads to the production of another second messenger inositol 1, 4, 5 triphosphate (IP_3). Some studies have shown that after pheromonal stimulation and application of phospholipase C blocker U73122, electrical activity, IP_3 production and calcium entry were blocked (Holy *et al.*, 2000; Spehr *et al.*, 2002).

The impact on signal transduction of Ca^{2+} entry facilitated by TRPC2 channels is still an open area for research. It has been shown that an increase in intracellular Ca^{2+} activates a Ca^{2+} activated nonselective cationic channel in hamster VSNs (Liman, 2003). Current was activated in both whole-cell and inside-out patches by using 2mM Ca^{2+}. This activated current was only permeable to Na^+ and K^+ ions and was blocked by ATP and cAMP in micromolar range, hence sharing the features with TRPM4 (Nilius & Vennekens, 2006). In another study, where current was elicited by applying 50µM Ca^{2+} in the inside-out patches, Ca^{2+} activated cationic conductance was also observed (Spehr *et al.*, 2009). The properties of these channels have not yet been investigated extensively (Spehr *et al.*, 2009). Till date it is unclear whether these channels contribute any role in the signal transduction pathway.

1.2.4.2 Generation of Action Potentials in Vomeronasal Sensory Neurons

Generation of action potentials is essential in VSNs to transfer the received information to the central areas. VSNs are equipped with many voltage-gated ion channels, which include voltage-gated sodium, potassium and calcium channels. These neurons fire action potentials either spontaneously, or in response to current

injections, or to appropriate stimuli (Liman & Corey, 1996; Fieni *et al.*, 2003; Shimazaki *et al.*, 2006; Holy *et al.*, 2000; Leinders-Zufall *et al.*, 2004).

Several VSNs show a repetitive firing behavior, tonically or in the presence of dilute urine, for up to 2-3 seconds without any sign of adaptation (Liman & Corey, 1996; Shimazaki *et al.*, 2006; Ukhanov *et al.*, 2007; Dibattista *et al.*, 2008; Lucas *et al.*, 2003; Zhang *et al.*, 2008). However, some studies showed that long stimulations of 10-60 seconds caused adaptation (Ukhanov *et al.*, 2007; Spehr *et al.*, 2009) and that this sensory adaptation requires influx of Ca^{2+} and is mediated by calmodulin (Spehr *et al.*, 2009).

After contact with stimuli, the signal transduction process in VSNs leads to the generation of an inward current that depolarizes the membrane until it reaches the firing threshold. Sodium channels are then activated and initiate the spike generation. The voltage-gated inward current is mainly a sodium current, composed of both TTX sensitive and TTX insensitive component (Liman & Corey, 1996; Fieni *et al.*, 2003; Shimazaki *et al.*, 2006; Ukhanov *et al.*, 2007). The average peak density of the current in the apical and basal neurons is different, while the activation and inactivation parameters were same in both types of neurons (Fieni *et al.*, 2003; Ukhanov *et al.*, 2007). Moreover, calcium spikes may play an important role in firing action potentials. Indeed, it has been shown that there are two current components related to the activity of voltage-gated calcium channel (Cav): a low voltage activated T-type current and an L-type current (Liman & Corey, 1996; Fieni *et al.*, 2003). In basal neurons the current density generated by these voltage-gated calcium channels is higher as compared to the apical neurons (Fieni *et al.*, 2003; Ukhanov *et al.*, 2007).

Repolarization of action potentials is carried out by the activation of various potassium channels, mainly by delayed rectifying potassium channels. Like the sodium current this potassium current is activated in the range of -40 to -50mV, but there is no significant difference as a function of holding potentials (Liman & Corey, 1996; Shimazaki *et al.*, 2006; Ukhanov *et al.*, 2007). Calcium activated potassium currents are also present in the VSNs. These outward rectifying currents

have peculiar N-shape current voltage relation and are blocked by Iberiotoxin and Charybdtoxin which are the specific inhibitors of BK channels.

1.3 Calcium-activated Chloride Currents

The transport of chloride ions through the cell membrane is tightly regulated by ion channels and transporters. Chloride channels are involved in many physiological processes, including: regulation of electrical excitability in neuronal cells, muscle contraction, secretion in different epithelial systems and sensory transduction. Chloride channels can be grouped into four categories: ligand- gated chloride channels, voltage- activated chloride channel, cAMP-regulate chloride channel and Ca^{2+}-activated chloride channels, CaCCs (Jentsch *et al.*, 2002).

Ca^{2+}-activated chloride currents were firstly described in *Xenopus laevis* oocyte (Barish, 1983; Miledi & Parker, 1984) and subsequently characterized in taste receptors cells, in photoreceptors, in various neuronal cell types, in smooth muscle cells and in airway and intestinal epithelial cells, in exocrine glands, in the kidney, in cardiac muscle cells and in endothelial cells (for review see Hartzell *et al*., 2005). This wide expression pattern suggests the involvement of CaCCs in numerous physiological processes.

Biophysical signatures of these channels include:

- They are activated by cytosolic Ca^{2+} with half maximal concentration for activation in submicromolar range (Huang *et al.*, 2012).
- They exhibit outward rectification at low intracellular Ca^{2+} concentration but display a linear current-voltage relation at higher intracellular Ca^{2+} concentration (Huang *et al.*, 2012).
- These channel allows the permeation of large anions, with the following typical ionic selectivity: NO_3^-> I^->Br^-> Cl^->F^- (Large & Wang, 1996; Qu & Hartzell, 2000; Huang *et al.*, 2012)

Until recently the molecular identity of CaCCs was unknown, limiting the possibility of a deep characterization of their physiological roles (see par. 1.3.4). Moreover, in many cellular systems, the values of the chloride equilibrium potential is still uncertain, and therefore the polarity and the amplitude of the chloride flux are unknown.

1.3.1 Molecular Candidates for CaCCs

An important step to understand the physiological role of CaCCs is to identify their molecular identity. Despite extensive studies of the biophysical and physiological properties of CaCCs, their molecular identification is a complex process. The main obstacle is the absence of a selective pharmacological agents that differentiate them from the other chloride channels. Some protein families which have been proposed to be CaCCs are listed below.

Calcium-Activated Chloride Channel Family (CLCA)

An early candidate for CaCC is the Ca^{2+}- activated chloride channel family (CLCA). These proteins were firstly purified from bovine trachea and named after calcium-dependent chloride conductance found in trachea and in other secretory epithelia (Cunningham *et al.,* 1995; Agnel *et al.,* 1999). Transfection in several cell types with cDNA encoding various CLCA proteins induce a Ca^{2+} -activated current (Elble *et al.,* 1997; Gandhi *et al.,* 1998; Gruber *et al.,* 1998; Pauli *et al.,* 2000), but there is a hesitancy to consider this as a CaCC because of its high homology with cell adhesion proteins (Pauli *et al.,* 2000; Gruber & Pauli 1998). Moreover, electrophysiological data such as calcium sensitivity, voltage sensitivity and pharmacology of CLCAs are not consistent with the properties of native CaCCs (Papassotiriou *et al.,* 2001). Indeed, electrophysiological characterization of bovine CLCA expressed in *X. laevis* oocyte and COS-7 cells (Cunningham *et al.,* 1995) have shown that Ca^{2+} -activated currents were similar to native CaCCs in terms of anionic selectivity but presented several other major discrepancies, including the following:

- In the absence of intracellular Ca^{2+}, CLCA currents recorded in oocytes could be activated only by depolarization.
- Currents were not blocked by niflumic acid (NFA), which has been shown to block the endogenous CaCCs.

- The current-voltage relationship of whole-cell current recorded in COS-7 cell was linear instead of outward rectifying.

Bestrophins

Bestrophin was first discovered as the gene responsible for Best vitelliform dystrophy (VMD2) (Petrukhin *et al.,* 1998). The first clear evidence that bestrophins are chloride channels was presented by Sun *et al.,* (2002) and Tsunenari *et al.* (2003). Mutagenesis studies have been performed to establish a direct link between protein and current (Qu *et al.,* 2004). Bestrophins are activated by physiological level of calcium which made them suitable candidates for CaCCs, however the biophysical properties of these channels recorded both by whole cell patch-clamp and excised patches did not reproduce all the features of native CaCCs, as detailed below:

- Native CaCCs exhibit voltage -dependent kinetics and outward rectification that are not seen in wild type human bestrophin-1 and mouse bestrophin-2 (Qu *et al.,* 2004 ; Tsunenari *et al.,* 2003; Hartzell *et al.,* 2008; Tsunenari *et al.,* 2006).
- In bestrophin-2 knockout mice, native Ca^{2+}-activated chloride currents in olfactory sensory neurons and submandibular salivary gland acinar cells remain unaffected (Pifferi *et al.,* 2009b; Romanenko *et al.,* 2010).
- Studies with bestrophin-2 knockout mice revealed that, in the colon, bestrophin-2 functions as a HCO^-_3 channel that localizes to the basolateral membrane of mucin secreting colonic goblet cells and not the chloride secreting enterocyte in mouse colon (Yu *et al.,* 2010)

In summary, evidences show that bestrophins can function as anion channels but probably not as the classic CaCCs.

TMEM16/Anoctamins

In 2008, three different laboratories discovered the same candidate, TMEM16A/anoctamin1, for the molecular identity of CaCCs, using different approaches (Yang *et al.*, 2008; Caputo *et al.*, 2008; Schroeder *et al.*, 2008). The term "TMEM16" comes from "Transmembrane proteins with unknown function 16", while anoctamin was used because these channels were anion selective and have eight putative transmembrane domains. Members of TMEM16 family is found throughout the eukaryotes including flies, yeast plants, mammals etc. Mammals have 10 genes while invertebrates possess lesser numbers.

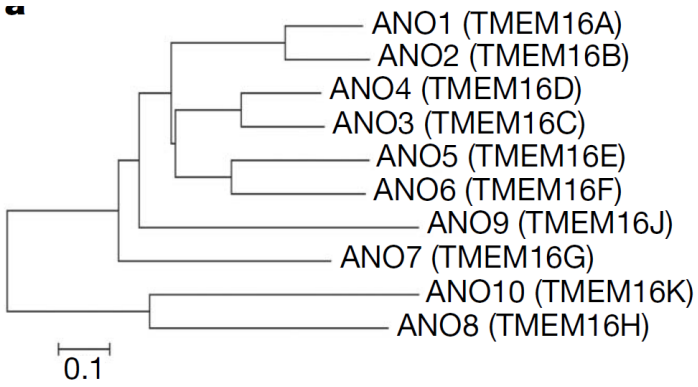

Fig 1.5: Phylogenetic tree depicting TMEM16 family in human *(*Yang *et al.*, 2008). Scale bar 0.1 nucleotide substitution per site.

1.3.2 TMEM16A and TMEM16B are CaCCs

Before the discovery of TMEM16A as a CaCC, this protein has gained the attention of many oncologists as it is overexpressed in many tumors. In 2008 TMEM16A enters in the scene. Three different approaches: bioinformatics analysis (Yang *et al.*, 2008), heterologous expression studies (Schroeder *et al.*, 2008) and functional genomics approach (Caputo *et al.*, 2008) in vivo, showed the possible role of TMEM16A as a CaCC. Interestingly it is seen that in different cell types TMEM16A generated Cl^- current having properties similar to native CaCCs.

The role of TMEM16A leads to the possibility that other members of the same family can also display the same properties of CaCC. In another study using the approach of *in-situ* hybridization it is seen that TMEM16B is expressed in mature olfactory sensory neurons (Yu *et al.,* 2005). The functional properties of native olfactory CaCC and TMEM16B in HEK-293 cells have shown remarkable similarities (Pifferi *et al.,* 2009; Stephan *et al.,* 2009). A more recent study also reported a side-by-side comparison obtained in whole-cell recordings with flash photolysis of caged Ca^{2+}, showing that the reversal potential for some external large anions changes with time, both in native olfactory CaCCs and in TMEM16B-induced currents in HEK 293 cells (Sagheddu *et al.,* 2010)

1.3.3 Structure and functional properties

It has been proposed that the tertiary structure of TMEM16A contains eight predicted transmembrane helices, intracellular NH_2- and COOH ends and a pore, formed by the 5th and 6th transmembrane helices together with a P-loop dipping back into the membrane (Fig. 1.6 left). However, in 2012 a study proposed an alternative model for TMEM16A. Their data contradict the popular re-entrant loop model by showing that the putative extracellular loop 4 (amino acids 650-706) is oriented intracellularly and may contain a Ca^{2+} binding site (Fig. 1.6 right) (Yu *et al.,* 2012). In this new model, the location of the pore forming domain is uncertain, as the authors could not localize the selectivity filter, so the true structure of TMEM16A still needs to be determined. It has been shown that TMEM16A does not exist as a single protein, but as obligate homodimer (Fallah *et al.,* 2011; Sheridan *et al.,* 2011).

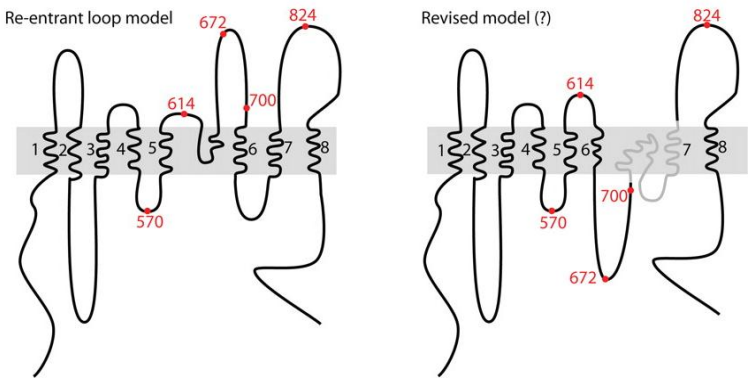

Fig 1.6: Topographical model of mTMEM16A (Yu *et al., 2012*)

1.3.3.1 Other TMEM16 members

Apart from TMEM16A and 16B, the role of other family members is uncertain. In a recent study it has been shown that some members of TMEM16 protein family do not produce robust current because they do not traffic to the plasma membrane. It was suggested that probably they have intracellular functions or they are missing necessary chaperone subunits to help them to reach the plasma membrane (Duran *et al.,* 2012).

Mutations in TMEM16E (also previously named GDD1) result in a musculoskeletal disorder. It is highly expressed in cardiac and skeletal muscle as well as in bones, and is greatly up-regulated during myocyte differentiation (Tsutsumi *et al.,* 2004).

TMEM16F plays an important role in blood clotting. Mutation in TMEM16F leads to Scott syndrome, a rare blood disorder caused by the defect in blood coagulation (Suzuki *et al.,* 2010). However there is no agreement about the function of TMEM16F. In one study it has been shown to act as a Ca^{2+}-activated cationic channel (Yang *et al.,* 2012) while in another study it has been shown to act like a anion channel with a delayed Ca^{2+}-activation (Grubb *et al.,* 2013).

TMEM16G is highly expressed in prostrate and was discovered in search for genes whose expression pattern mimicked those of known prostate cancer genes (Bera *et al.,* 2004; Das *et al.,* 2007). The role of TMEM16G has been suggested as a cell association protein (Das *et al.,* 2007). Mutation in TMEM16K have been linked to

autosomal recessive cerebral ataxia with moderate gait ataxia, down beat nystagmus and dysarthic speech (Vermeer *et al.,* 2010). Affected individual show severe cerebellar atrophy.

1.3.4 Physiological Roles of Calcium-activated Chloride Currents

Ca^{2+}-activated currents have been recorded in various cell types and their physiological significance has been the object of much investigation and speculation (Hartzell *et al.,* 2005). Three factors command the trend of chloride movement through CaCCs. These factors include, the membrane potential, the Cl^- concentration gradient and the $[Ca^{2+}]_i$.

CaCCs are expressed in different neurons including dorsal root ganglion (DRG), spinal cord neurons and autonomic neurons. In most of the cases these channels are not present among all the neuronal population but in distinct subsets, which suggests the specific function of these neurons. About 45-90% of the neurons in DRG express CaCCs (Bader *et al.,* 1987; Scott *et al.,* 1988; Stapleton *et al.,* 1994; Currie *et al.,* 1995). It has been proposed that the CaCCs in DRG are responsible for after-depolarization following action potentials (Mayer, 1985; De Castro *et al.,* 1987). CaCCs are also expressed in spinal cord neurons (Hussy, 1991; Hussy 1991). Only a fraction of spinal cord neurons expresses CaCCs (Frings *et al.,* 2000).

CaCCs have a long evolutionary history from the propagation of action potential in algae to Xenopus oocytes, where the rapid efflux of Cl^- through these channels after the encounter with sperm, prevents the polyspermy (Cross, 1981). They are also present in mammalian excitable cells, for example the interstitial cells of Cajal where CaCC leads to the generation of a slow wave leading to the gastrointestinal tract peristalsis (Sanders *et al.,* 2006).

The airway epithelium uses ion transport mechanisms to control the level of airway surface liquid which is important for hydration and protection against infection (Hartzell *et al.,* 2005). The transporters which are located on the basal surface are responsible to accumulate the chloride in the cell while CaCCs and Cystic Fibrosis tansport regulator (CFTR) are expressed in the apical surface.The interplay between CaCC and CFTR regulate the airways mucous layer.

In olfactory sensory neurons Cl^- efflux through the CaCC leads to the further amplification of the initial signal. It has been estimated that the magnitude of initial current is increased up to 30 times to that of the initial response hence increasing the signal to noise ratio which in turns increase the sensitivity to odorants (Kurahashi & Kaneko, 1991; Kleene, 2008).

CaCCs are present in both mammalian and amphibian taste receptors (McBride & Roper, 1991; Herness & Sun, 1999). In Necturus, action potential are followed by an outward current that is mediated by CaCCs which open in response to Ca^{2+} influx during the action potential (McBride & Roper, 1991; (Taylor & Roper, 1994).

Aim

The aim of this study is to investigate the physiological role played by the increase in intracellular Ca^{2+} concentration in mouse vomeronasal sensory neurons. We used a combination of electrophysiological and immunohistochemistry techniques to identify Ca^{2+}-activated chloride channels responsible for such currents. Ca^{2+} inside neurons was increased by flash photolysis of caged Ca^{2+} in the apical region of vomeronasal sensory neurons, or by increasing the calcium concentration in the intracellular solution in the patch pipette.

Materials and Methods.

Materials and methods used in Dibattista *et al*. 2012 are described in the article reported in the Result section of this thesis.

Preparation of isolated VSNs.

All animals were handled in accordance with the Italian Guidelines for the Use of Laboratory Animals (DecretoLegislativo 27/01/1992, no. 116) and European Union guidelines on animal research (no. 86/609/EEC). For experiments, 2-months-old mice were anaesthetized by CO_2 inhalation and decapitated before VNO removal. The vomer capsule containing the VNO was removed as described previously (Liman and Corey, 1996; Dean *et al*., 2004; Shimazaki *et al*., 2006; Arnson *et al.*, 2010), and VSNs were dissociated from the VNO with a standard enzymatic–mechanical dissociation protocol (Dibattista *et al.*, 2008). In brief, the removed vomer capsule was rapidly transferred to a Petri dish containing divalent-free PBS (Sigma-Aldrich) solution where the VNO was extracted. The tissue was cut into small pieces with tiny scissors, transferred to divalent-free PBS containing 1 mg/ml collagenase (type A), incubated at 37°C for 10 min, cut into small pieces with tiny scissors, and reincubated for 10 min at 37°C. After a 2-min centrifugation at 1,200 rpm, the tissue was gently triturated with a fire-polished Pasteur pipette. Cells were suspended in 1 ml of fresh Ringer's solution and plated on Nunc dishes (World Precision Instruments) were coated with poly-L-lysine and concanavalin A (type V; Sigma-Aldrich). Cells were stored at 4°C for up to 7 hours before experiments.

Electrophysiological recordings and ionic solutions

Current recordings from isolated VSNs were performed in the whole-cell voltage-clamp configuration, as described previously (Dibattista *et al* 2012; Sagheddu *et al.*, 2010). Patch pipettes were made of borosilicate glass (World Precision Instruments, Inc.) and pulled with a PP-830 puller (Narishige). Patch pipettes filled with the intracellular solution had a resistance of 3–5 MΩ when immersed in the bath solution. Currents were recorded Axopatch 200B amplifier controlled by Clampex 10 via a Digidata 1440 (Molecular Devices). Data were low-pass filtered at 5 kHz and sampled at 10 kHz. Experiments were performed at room temperature (20–25°C). The standard extracellular solution contained (in mM): 140 NaCl, 5 KCl, 2 $CaCl_2$, 1 $MgCl_2$, 10 glucose, and 10 HEPES, adjusted to pH 7.4 with NaOH. The intracellular solution filling the patch pipette contained (in mM): 140 CsCl, 10 HEPES, and 10 HEDTA, adjusted to pH 7.2 with CsOH, and no added Ca^{2+} for the nominally 0 Ca^{2+} solution, or various added Ca^{2+} concentrations, as calculated with the program WinMAXC (Patton *et al*., 2004), to obtain free Ca^{2+} in the range between 0.5 and 1.5 μM. For 2 mM Ca^{2+} the intracellular solution contained (in mM) 145 NaCl, 10 Hepes, 2 $CaCl_2$ as in Liman (2003). The free Ca^{2+} concentrations were experimentally determined by Fura-4F (Invitrogen) measurements by using a luminescence spectrophotometer (LS-50B; PerkinElmer), as described previously (Pifferi *et al*., 2006). All chemicals, unless otherwise stated, were purchased from Sigma-Aldrich. In most experiments, we applied voltage steps of 200-ms duration from a holding potential of 0 mV ranging from -100 to +100 mV (or from -100 to +160 mV), followed by a step to -100 mV. In another set of experiments, channels were activated by a 200-ms pulse to +100 mV, and then rapidly closed by the application of hyperpolarizing steps.

For ionic selectivity experiments, NaCl was replaced with equimolar Choline-Cl, or Cl^- was substituted with other anions, such as isothiocyanate (SCN^-) or gluconate. The 1mM Cl solution contained (in mM): 1 NaCl, 139 Na-Gluconate, 2.5 K_2SO_4, 2 $CaSO_4$, 1 $MgSO_4$, 10 glucose, and 10 HEPES, adjusted to pH 7.4 with NaOH. The bath was grounded through a 3M KCl Agar Bridge connected to an Ag-AgCl reference electrode.

NFA was prepared in DMSO as stock solutions at 200 mM and diluted to the final concentration of 300 µM. $CaCC_{inh-A01}$ was also dissolved in DMSO at a stock solution 20mM and diluted in Ringer to get a final concentration of 10 µM.

Bathing solutions were changed by using a gravity-fed perfusion system with a slow perfusion rate, adjusted in such a way that the position of the neuron was not perturbed. A complete solution change was obtained in ∼10 s. To measure blocker effects, current recordings were obtained before blocker application until a stable response was obtained (control), 2 min after delivery of the solution with the blocker, and 2–5 min after perfusion with Ringer's solution without the blocker (wash).

Data analysis

Data are presented as mean $\pm$ SEM, with *n* indicating the number of cells. Data analysis and figures were made with Igor Pro software (WaveMetrics).

Results

1. Calcium-activated chloride channels in the apical region of mouse vomeronasal sensory neurons

Dibattista M, **Amjad A**, Maurya DK, Sagheddu C, Montani G, Tirindelli R, Menini A (2012)

Article

Calcium-activated chloride channels in the apical region of mouse vomeronasal sensory neurons

Michele Dibattista,[1] Asma Amjad,[1] Devendra Kumar Maurya,[1] Claudia Sagheddu,[1] Giorgia Montani,[2] Roberto Tirindelli,[2] and Anna Menini[1]

[1]Neurobiology Sector and Italian Institute of Technology Unit, Scuola Internazionale Superiore di Studi Avanzati (SISSA), 34136 Trieste, Italy

[2]Department of Neuroscience, University of Parma, and Brain Center for Social and Motor Cognition, Italian Institute of Technology, 43121 Parma, Italy

The rodent vomeronasal organ plays a crucial role in several social behaviors. Detection of pheromones or other emitted signaling molecules occurs in the dendritic microvilli of vomeronasal sensory neurons, where the binding of molecules to vomeronasal receptors leads to the influx of sodium and calcium ions mainly through the transient receptor potential canonical 2 (TRPC2) channel. To investigate the physiological role played by the increase in intracellular calcium concentration in the apical region of these neurons, we produced localized, rapid, and reproducible increases in calcium concentration with flash photolysis of caged calcium and measured calcium-activated currents with the whole cell voltage-clamp technique. On average, a large inward calcium-activated current of −261 pA was measured at −50 mV, rising with a time constant of 13 ms. Ion substitution experiments showed that this current is anion selective. Moreover, the chloride channel blockers niflumic acid and 4,4′-diisothiocyanatostilbene-2,2′-disulfonic acid partially inhibited the calcium-activated current. These results directly demonstrate that a large chloride current can be activated by calcium in the apical region of mouse vomeronasal sensory neurons. Furthermore, we showed by immunohistochemistry that the calcium-activated chloride channels TMEM16A/anoctamin1 and TMEM16B/anoctamin2 are present in the apical layer of the vomeronasal epithelium, where they largely colocalize with the TRPC2 transduction channel. Immunocytochemistry on isolated vomeronasal sensory neurons showed that TMEM16A and TMEM16B coexpress in the neuronal microvilli. Therefore, we conclude that microvilli of mouse vomeronasal sensory neurons have a high density of calcium-activated chloride channels that may play an important role in vomeronasal transduction.

INTRODUCTION

Many social behaviors in animals are triggered by molecules with various chemical structures. In mammals, several chemosensory organs, such as the main olfactory epithelium, the vomeronasal organ (VNO), the septal organ, and the Grüneberg ganglion, are involved in chemical detection (Brennan and Zufall, 2006; Zufall and Leinders-Zufall, 2007; Brennan, 2009; Ma, 2009; Munger et al., 2009; Tirindelli et al., 2009; Touhara and Vosshall, 2009). Among these, the two main systems are represented by the main olfactory epithelium and the VNO. In both sensory systems, signal transduction occurs in bipolar sensory neurons and leads to membrane depolarization, although different transduction cascades are involved.

In most olfactory sensory neurons of the main olfactory epithelium, signal transduction occurs in the cilia protruding from the neurons' apical surface. The binding of molecules to odorant receptors leads to cAMP production and to the opening of CNG channels in the ciliary membrane. Na^+ and Ca^{2+} influx through CNG channels produces a depolarization of the neuron, and the increase in cytoplasmic Ca^{2+} concentration in the cilia has several effects, including a role in adaptation and the activation of Cl^- channels (Schild and Restrepo, 1998; Pifferi et al., 2006, 2009b; Kleene, 2008; Frings, 2009a,b; Reisert and Zhao, 2011).

In most vomeronasal sensory neurons, signal transduction occurs in microvilli that are present at the neurons' apical surface. The binding of molecules to vomeronasal receptors activates a phospholipase C signaling cascade, leading to the opening of ion channels that allow Na^+ and Ca^{2+} influx. The transient receptor potential canonical 2 (TRPC2) channel is expressed in the neurons' microvilli (Liman et al., 1999) and is mainly responsible for such cation influx (Zufall et al., 2005;

Correspondence to Anna Menini: menini@sissa.it

M. Dibattista's present address is Monell Chemical Senses Center, Philadelphia, PA 19104.

Abbreviations used in this paper: DAPI, 4′-6-diamidino-2-phenylindole; DIDS, 4,4′-diisothiocyanatostilbene-2,2′-disulfonic acid; MeS^-, methanesulfonate; NFA, niflumic acid; PDE4A, phosphodiesterase 4A; SCN^-, isothiocyanate; TRPC2, transient receptor potential canonical 2; VNO, vomeronasal organ.

The Rockefeller University Press $30.00
J. Gen. Physiol. Vol. 140 No. 1 3–15
www.jgp.org/cgi/doi/10.1085/jgp.201210780

Munger et al., 2009). Several studies demonstrated that vomeronasal sensory neurons respond to stimuli with the generation of action potentials and an increase in intracellular Ca^{2+} concentration (Holy et al., 2000; Leinders-Zufall et al., 2000, 2004, 2009; Spehr et al., 2002; Chamero et al., 2007). However, the role played by cytoplasmic Ca^{2+} elevation in the microvilli is still largely unknown. Spehr et al. (2009) have recently shown that Ca^{2+} in combination with calmodulin is responsible for sensory adaptation. In addition, other studies suggested that intracellular Ca^{2+} might also activate ion channels involved in the transduction process, although it is still a matter of debate whether these channels are cation or anion selective. Indeed, Ca^{2+}-activated nonselective cation currents have been measured in hamster (Liman, 2003) or mouse vomeronasal sensory neurons (Spehr et al., 2009). In the whole cell configuration, currents of about −177 pA at −80 mV were activated by dialysis of 0.5 or 2 mM Ca^{2+} (Liman, 2003). In excised inside-out patches, the dose–response relation indicated that half-activation of the channels occurred at 0.5 mM Ca^{2+} at −80 mV (Liman, 2003). It has been suggested that this Ca^{2+}-activated nonselective cation channel could directly mediate vomeronasal sensory transduction or amplify the primary sensory response (Liman, 2003), but at present its role and its molecular identity are still unknown. Other studies suggested that a significant portion of the response to urine in mouse vomeronasal sensory neurons is carried by Ca^{2+}-activated Cl^- channels (Yang and Delay, 2010; Kim et al., 2011). However, these studies used indirect ways to activate channels, as the increase in cytoplasmic Ca^{2+} concentration was a secondary effect of urine stimulation.

Thus, at present, it is still unclear whether nonselective cation and/or Cl^- channels activated by Ca^{2+} are expressed in the apical region of vomeronasal sensory neurons and may be involved in vomeronasal transduction. To contribute to the resolution of this debate, we directly recorded and characterized currents by producing rapid and repeatable increases in intracellular Ca^{2+} concentration using flash photolysis of caged Ca^{2+}, while recording the induced current in the whole cell voltage-clamp configuration (Boccaccio et al., 2011). The use of photolysis of caged Ca^{2+} to produce an increase in Ca^{2+} concentration, instead of dialysis of Ca^{2+} into the neuron or the production of a secondary Ca^{2+} increase, allowed us to release Ca^{2+} in a temporally and spatially defined manner into an intact neuron because we could precisely deliver a flash of UV light at the apical region of a vomeronasal sensory neuron. We measured an average inward Ca^{2+}-activated current of −261 pA at the holding potential of −50 mV and showed that this current is anion selective. Furthermore, both niflumic acid (NFA) and 4,4′-diisothiocyanatostilbene-2,2′-disulfonic acid (DIDS), two very well known Cl^- channel blockers (Frings et al., 2000; Hartzell et al., 2005), partially blocked the Ca^{2+}-activated current in vomeronasal sensory neurons.

To the best of our knowledge, these are the first recordings providing a direct demonstration that a large Cl^- current can be directly activated by Ca^{2+} in the apical region of mouse vomeronasal sensory neurons, as this demonstration can only be obtained by using a method that provides a temporal and spatial control of Ca^{2+} release, such as photolysis of caged Ca^{2+}.

Recent studies indicated that at least two members of the TMEM16/anoctamin family, TMEM16A/anoctamin1 and TMEM16B/anoctamin2, are Ca^{2+}-activated Cl^- channels (Caputo et al., 2008; Schroeder et al., 2008; Yang et al., 2008; Pifferi et al., 2009a, 2012; Stephan et al., 2009; Stöhr et al., 2009; Scudieri et al., 2012). We studied the expression of members of this family in the VNO and found that both TMEM16A and TMEM16B are expressed in the apical region of the VNO, in agreement with recent studies (Rasche et al., 2010; Billig et al., 2011; Dauner et al., 2012). However, microvilli both from vomeronasal sensory neurons and from supporting cells are present at the apical surface of the vomeronasal epithelium, and they are not clearly distinguishable. We therefore investigated the localization of TMEM16A and TMEM16B in isolated vomeronasal sensory neurons and found that these channels are expressed in neurons' microvilli. Because microvilli are the site where transduction events take place, the presence of Ca^{2+}-activated Cl^- channels indicates that they may be involved in signal transduction in the VNO. A complete understanding of conductances present in vomeronasal sensory neurons will help to elucidate the molecular mechanisms involved in the generation of the vomeronasal transduction current and the production of action potentials.

MATERIALS AND METHODS

Preparation of isolated vomeronasal sensory neurons

All animals were handled in accordance with the Italian Guidelines for the Use of Laboratory Animals (Decreto Legislativo 27/01/1992, no. 116) and European Union guidelines on animal research (no. 86/609/EEC). For experiments, 2-mo-old mice were anaesthetized by CO_2 inhalation and decapitated before VNO removal. The vomer capsule containing the VNO was removed as described previously (Liman and Corey, 1996; Dean et al., 2004; Shimazaki et al., 2006; Arnson et al., 2010), and vomeronasal sensory neurons were dissociated from the VNO with a standard enzymatic–mechanical dissociation protocol (Dibattista et al., 2008). In brief, the removed vomer capsule was rapidly transferred to a Petri dish containing divalent-free PBS (Sigma-Aldrich) solution where the VNO was extracted. The tissue was cut into small pieces with tiny scissors, transferred to divalent-free PBS containing 1 mg/ml collagenase (type A), incubated at 37°C for 10 min, cut into small pieces with tiny scissors, and reincubated for 10 min at 37°C. After a 2-min centrifugation at 1,700 rpm, the tissue was gently triturated with a fire-polished Pasteur pipette. Cells were resuspended in 1 ml of fresh Ringer's solution and plated on a glass coverslip (World Precision

Instruments) coated with poly-L-lysine and concanavalin A (type V; Sigma-Aldrich). Cells were stored at 4°C for up to 7 h before experiments.

Patch-clamp recordings

Vomeronasal sensory neurons were observed using an inverted microscope (IX 70; Olympus) with an oil immersion ×100 objective (Carl Zeiss). Currents in whole cell voltage-clamp configuration were recorded using an Axopatch 200B patch-clamp amplifier controlled by Clampex 8 connected with a Digidata 1322A (Molecular Devices). Patch pipettes were made using borosilicate capillaries (World Precision Instruments) and were pulled by a two-stage vertical puller (PP-83; Narishige). Pipette resistance was around 3–6 MΩ. Currents were low-pass filtered at 1 kHz and acquired at 2 kHz. All the experiments were performed at room temperature (20–24°C).

Ionic solutions, photolysis of caged Ca^{2+}, and perfusion system

The extracellular mammalian Ringer's solution contained (in mM): 140 NaCl, 5 KCl, 1 $CaCl_2$, 1 $MgCl_2$, 10 HEPES, 10 glucose, and 1 sodium pyruvate, pH 7.4. For flash photolysis of caged compounds, we used a xenon flash–lamp system (JML-C2; Rapp OptoElectronic) coupled with the epifluorescence port of the inverted microscope with a quartz light guide, as described previously (Boccaccio et al., 2006, 2011; Boccaccio and Menini, 2007). The light spot had a diameter of ∼15 µm and was focused on the microvilli and dendritic knob of isolated vomeronasal sensory neurons. The flash duration was <1.5 ms and was kept constant for each experiment. The interval between flashes was at least 2 min. At the beginning of each experiment, the stability of the response was checked by applying repetitive flashes at intervals of 2 min. Neurons that did not reach a stable response to at least two consecutive flashes were discarded.

The intracellular recording solution for the photorelease of caged Ca^{2+} contained (in mM): 3 DMNP-EDTA, 1.5 $CaCl_2$, 140 CsCl, and 10 HEPES, pH 7.4. DMNP-EDTA was purchased from Invitrogen, and $CaCl_2$ was adjusted with a 0.1-M standard solution from Fluka. Aliquots were stored at −20°C and kept refrigerated in the dark during the experiment.

For ionic selectivity experiments, NaCl was replaced with equimolar NMDG-Cl, or Cl^- was substituted with other anions, such as methanesulfonate (MeS^-) or isothiocyanate (SCN^-), by replacing NaCl on an equimolar basis with NaX, where X is the substituted anion.

The bath was grounded through a 1-M KCl agar bridge connected to an Ag-AgCl reference electrode. Liquid junction potentials were calculated using the Clampex's Junction Potential Calculator (Molecular Devices), based on the JPCalc program developed by Barry (1994), and applied membrane potentials were corrected offline for the calculated liquid junction potentials, as described previously (Sagheddu et al., 2010).

NFA was prepared in DMSO as stock solutions at 200 mM and diluted to the final concentration of 300 µM. DMSO alone did not modify the currents. DIDS was directly dissolved in the bathing solution to 1 mM.

Bathing solutions were changed by using a gravity-fed perfusion system with a slow perfusion rate, adjusted in such a way that the position of the neuron was not perturbed. A complete solution change was obtained in ∼10 s. To measure blocker effects, current recordings were obtained before blocker application until a stable response was obtained (control), 2 min after delivery of the solution with the blocker, and 2–5 min after perfusion with Ringer's solution without the blocker (wash).

Chemicals, unless otherwise stated, were purchased from Sigma-Aldrich.

Analysis of electrophysiological data

Data analysis and figures were made using Clampfit and IGOR software (WaveMetrics). Current recordings at each holding potential were plotted by subtracting the value of the baseline measured before photorelease of caged Ca^{2+}. Data are given as mean ± SEM and the total number of neurons (n). Statistical significance was tested with a Student's t test. $P < 0.05$ was considered statistically significant.

RNA extraction and RT-PCR

RNA was extracted from the VNO of FVB mice. Methods and primers for the amplification of TMEM16/anoctamins cDNA were the same as described previously (Sagheddu et al., 2010). All amplicons were gel extracted, subcloned, and sequenced for confirmation.

Immunofluorescence

HEK 293T cells were grown on coverslips and cotransfected with plasmids containing the cDNA sequence of TMEM16A or TMEM16B (RZPD) and enhanced GFP (Takara Bio Inc.) for fluorescent identification of transfected cells, as described previously (Pifferi et al., 2009a). Transfected cells were fixed in 4% paraformaldehyde for 15 min at room temperature and sequentially washed. Next, they were incubated with a quenching solution (0.1 M glycine) for 10 min and then treated with 0.05% SDS for antigen retrieval for 10 min. Cells were subsequently incubated for 15 min in blocking solution (2% [vol/vol] FBS and 0.2% [vol/vol] Triton X-100 in PBS), followed by incubation with the primary antibody for 3 h at 4°C. After washing with PBS-T (0.1% Tween 20 in PBS), cells were incubated for 45 min with the secondary antibody, prepared in PBS-T. Finally, cells were incubated with 0.1 µg/ml 4′-6-diamidino-2-phenylindole (DAPI) for 15 min, and coverslips were mounted with Vectashield (Vector Laboratories).

For immunohistochemistry on tissue sections, the mouse nasal regions or the VNOs extracted from the nasal cavity were fixed in 4% paraformaldehyde (for 4 h at 4°C), then decalcified in 0.5 M EDTA for 12 h at 4°C, and subsequently equilibrated overnight (4°C) in 30% (wt/vol) sucrose for cryoprotection. 14-µm coronal sections were cut with a cryostat and stored (−80°C) for further use. For antigen retrieval, sections were treated with SDS 0.5% (wt/vol) in PBS for 15 min. Sections were incubated in a blocking solution (2% [vol/vol] FBS and 0.2% [vol/vol] Triton X-100 in PBS) for 2 h, and then with the primary antibody (diluted in the blocking solution) overnight at 4°C. Sections were then rinsed with 0.1% (vol/vol) Tween 20 in PBS (PBS-T) and incubated with the fluorophore-conjugated secondary antibody (diluted in PBS-T) for 2 h at room temperature. After washing with PBS-T, sections were treated with 0.1 µg/ml DAPI for 30 min, washed with PBS-T, and mounted with Vectashield (Vector Laboratories).

Immunocytochemistry on isolated vomeronasal sensory neurons was performed as described previously (Fieni et al., 2003). Dissociated vomeronasal sensory neurons were prepared as for electrophysiological experiments. Glass-attached vomeronasal neurons were gently perfused with 4% paraformaldehyde and then washed in PBS. Cells were blocked in 1% albumin and 0.3% Triton X-100 in PBS for 20 min and incubated overnight with the primary antibody. Cells were then washed in PBS and further incubated with the secondary antibody, prepared in PBS. In some experiments, cells were also incubated with 0.1 µg/ml DAPI for 15 min. Coverslips were mounted with Vectashield (Vector Laboratories).

Wild-type C57BL6 or genetically modified mice that express GFP in all mature olfactory and vomeronasal sensory neurons (OMP-GFP mice; provided by P. Mombaerts, Max Planck Institute of Biophysics, Frankfurt, Germany) were used.

The following primary antibodies were used: rabbit anti-TMEM16A (1:50; Abcam), rabbit anti-TMEM16B (1:100; Santa Cruz Biotechnology, Inc.), guinea pig anti-TMEM16A and guinea

pig anti-TMEM16B (provided by S. Frings, Heidelberg University, Heidelberg, Germany; Dauner et al., 2012), goat anti-TRPC2 (1:50; Santa Cruz Biotechnology, Inc.), rabbit anti-Gαo (1:100; Santa Cruz Biotechnology, Inc.), and rabbit anti–phosphodiesterase 4A (PDE4A; 1:50; Abcam). The following secondary antibodies, obtained from Invitrogen, were used: goat anti–guinea pig Alexa Fluor 594 (1:500), goat anti–rabbit Alexa Fluor 488 (1:500), goat anti–rabbit Alexa Fluor 594 (1:500), goat anti–rabbit Alexa Fluor 405 (1:500), chicken anti–rabbit Alexa Fluor 594 (1:500), and chicken anti–goat Alexa Fluor 488 (1:500).

Immunoreactivity was visualized with a confocal microscope (TCS SP2; Leica). Images were acquired using Leica software (at 1,024 × 1,024–pixel resolution) and were not modified other than to balance brightness and contrast. Control experiments without the primary antibodies gave no signal.

RESULTS

Whole cell currents activated by photolysis of caged Ca^{2+} at the apical region of mouse vomeronasal sensory neurons

We obtained whole cell voltage-clamp recordings from isolated mouse vomeronasal sensory neurons and directly measured Ca^{2+}-activated currents by rapidly elevating the Ca^{2+} concentration in the apical region (dendritic knob and microvilli) by localized photorelease of caged Ca^{2+} (Fig. 1 A). Fig. 1 B shows a typical current response at the holding potential of −50 mV. An inward current rapidly developed upon the flash release, reaching a peak amplitude of −508 pA, and then slowly returned to baseline. The rising phase of the Ca^{2+}-activated current was well described by a single-exponential function with a time constant of 9.5 ms (Fig. 1 C). Similar results were obtained from a total of 59 neurons with an average time constant value of 12.6 ± 6.0 ms (n = 59; range of 3–26 ms). We observed a large variability in Ca^{2+}-activated current amplitudes in different neurons with absolute values ranging between 50 pA and 1 nA at −50 mV, and a mean amplitude of −261 ± 37 pA (n = 59). Such variability has also been observed in recording Ca^{2+}-activated currents in the ciliary region of olfactory sensory neurons, where absolute values ranging from 50 pA up to ∼1 nA were also recorded (Boccaccio et al., 2006; Boccaccio and Menini, 2007). The amplitude variability can originate both from the illumination conditions in the neuron that may differ between experiments as well as from various numbers or densities of channels that may vary in different neurons. Similarly to olfactory sensory neurons, we also found a large variability in the time necessary for the current to return to baseline in vomeronasal sensory neurons (Figs. 1 B and 3, A and B). This is likely to be the result of differences in the time necessary for the decrease in Ca^{2+} concentration by Ca^{2+} extrusion and/or by diffusion to other neuronal compartments.

To investigate the ionic nature of the Ca^{2+}-activated currents, we measured the reversal potential in various ionic conditions. Currents were recorded at various holding potentials with different ionic compositions in the extracellular solution. In a first set of experiments, we used our standard intracellular and extracellular solutions, in which Cs^+ was chosen as the intracellular monovalent cation to avoid contributions from Ca^{2+}-activated K^+ currents, and Na^+ was the main extracellular monovalent cation. Moreover, the intracellular and extracellular Cl^- concentrations were almost symmetrical. Fig. 2 A shows the responses induced by photorelease of Ca^{2+} at the indicated holding potentials. The reversal potential calculated from the current–voltage relation was +0.5 mV, with an average value of +0.3 ± 3.5 mV (n = 6; Fig. 2 E). Because the cation concentrations were $[Na^+]_o$ = 149 mM and $[Cs^+]_i$ = 143 mM, and the Cl^- concentrations were $[Cl^-]_o$ = 149 mM and $[Cl^-]_i$ = 143 mM, a reversal potential value close to 0 mV is consistent both with a nonselective cation current and with an anion-selective current.

To distinguish between the two types of currents, we performed a first set of experiments by replacing Na^+ in the extracellular solution with $NMDG^+$, a large organic monovalent cation largely impermeant in cation channels. If the measured Ca^{2+}-activated currents were carried by cations, the replacement of Na^+ by $NMDG^+$ should produce a shift of the reversal potential toward negative values. Fig. 2 B shows that the reversal potential in the presence of 140 mM NMDG-Cl was +0.3 mV, with an average value of +0.5 ± 3.8 mV (n = 3; Fig. 2 E), indicating that the Ca^{2+}-activated current was not carried by cations.

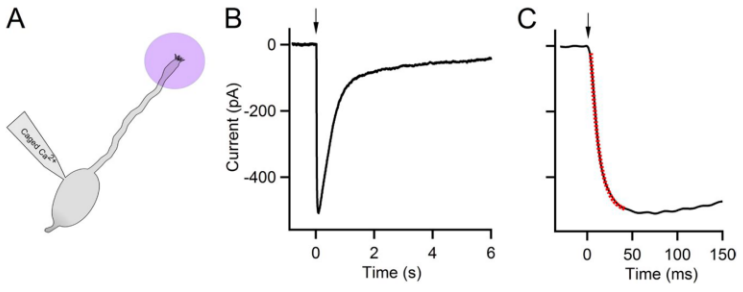

Figure 1. Current responses induced by photorelease of Ca^{2+} in the apical region of mouse vomeronasal sensory neurons. (A) Schematic drawing of a vomeronasal sensory neuron showing the location of application of the UV flash to photorelease Ca^{2+}. (B) Whole cell current induced by photorelease of Ca^{2+} at the holding potential of −50 mV. A flash was applied at time t = 0 (indicated by an arrow). (C) Expanded timescale shows the rapid increase in the current upon Ca^{2+} photorelease. The current rising phase was well fitted by a single exponential (red dotted line) with a τ value of 9.5 ms.

In a second set of experiments, we tested whether the Ca^{2+}-activated current was carried by Cl^- by substituting most of the extracellular Cl^- with MeS^-, an anion known to be almost impermeant in Cl^- channels. Fig. 2 C shows that, when we replaced 140 NaCl with NaMeS, the reversal potential was +18 mV, with an average value of +20.2 ± 1.5 mV (n = 3; Fig. 2 E). The average reversal potential in the low extracellular Cl^- solution was shifted toward more positive values, as expected if MeS^- is much less permeant than Cl^-. Furthermore, because most Cl^- channels are more permeable to SCN^- than to Cl^-, we measured the reversal potential after replacing 140 mM NaCl with NaSCN: the reversal potential shifted toward more negative values, −20 mV (Fig. 2 D), with an average value of −18 ± 3 mV (n = 8; Fig. 2 E). These results demonstrate that the Ca^{2+}-activated current is an anion current and that these ion channels have higher permeability for SCN^- over Cl^-, as in most Cl^- channels (Hartzell et al., 2005).

To further characterize these channels, we measured the extracellular blockage by NFA and DIDS, two compounds commonly used to partially block Ca^{2+}-activated Cl^- currents in various tissues (Frings et al., 2000). Fig. 3 A shows the blocking effect by 300 µM NFA of the current elicited by photolysis of caged Ca^{2+} at −50 mV. The maximal inward current decreased from −1,022 to −221 pA upon NFA application, corresponding to 22% of its value before blocker application. The blocking effect was partially reversible after perfusion with Ringer's solution without NFA, as the current amplitude recovered to −505 pA, 50% of the control value. On average, the current amplitude in the presence of 300 µM NFA at −50 mV was 27% (n = 5) of the value before blocker application (Fig. 3 C). After perfusion with Ringer's

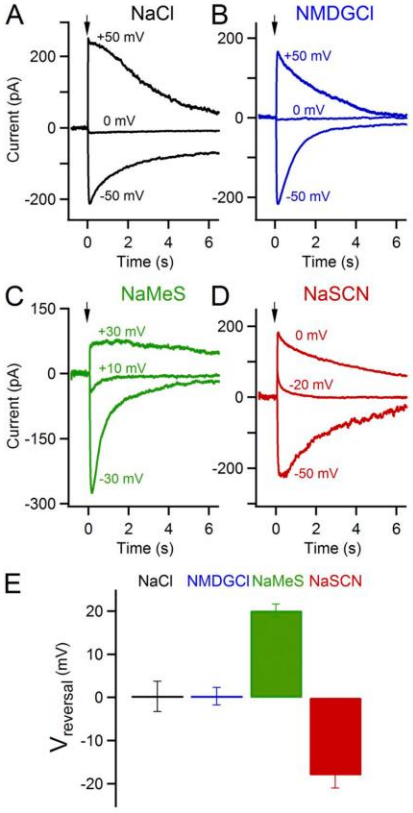

Figure 2. Ion selectivity of the Ca^{2+}-activated current. Whole cell currents from vomeronasal sensory neurons induced by photorelease of Ca^{2+} into the apical region recorded at the indicated holding potentials. A UV flash was applied at the time t = 0 (indicated by an arrow). Recordings in the presence of extracellular Ringer's solution containing 140 mM: (A) NaCl, (B) NMDG-Cl, (C) NaMeS, and (D) NaSCN, each from a different neuron. (E) Average reversal potentials measured in the presence of the indicated ionic solutions: NaCl (n = 6), NMDG-Cl (n = 3), NaMeS (n = 3), and NaSCN (n = 8).

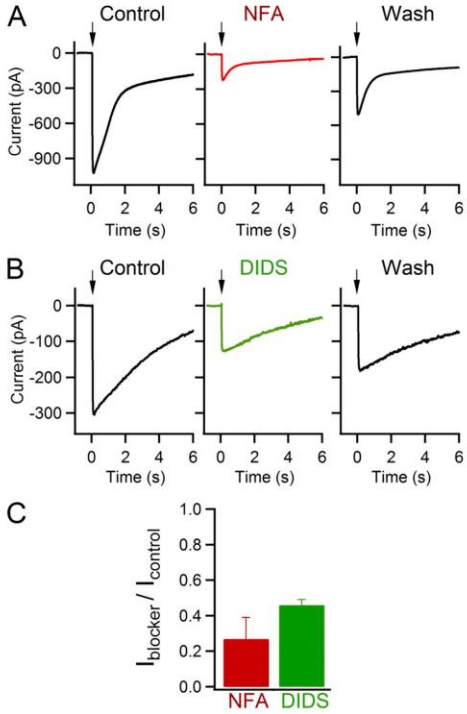

Figure 3. Blockage of the Ca^{2+}-activated Cl^- current. Whole cell currents induced by photorelease of Ca^{2+} into the apical region of vomeronasal sensory neurons. The holding potential was −50 mV. Current recordings were obtained before blocker application (control), 2 min after application of the indicated blockers, and 2 min after the removal of blockers (wash). The following blockers were used: (A) 300 µM NFA and (B) 1 mM DIDS. (C) Average values of the current in the presence of 300 µM NFA (n = 5) or 1 mM DIDS (n = 3) normalized to the current in control conditions ($P < 0.05$).

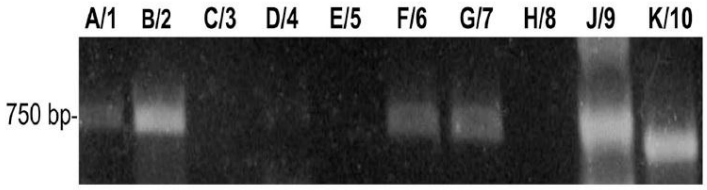

Figure 4. Expression of TMEM16s/anoctamins in mouse VNO. TMEM16/anoctamin isoforms A–J (1–10) were amplified from VNO cDNA by RT-PCR. A/1, B/2, F/6, G/7, J/9, and K/10 are expressed in the VNO.

solution without the blocker, the current recovered on average to 68% of its control value.

Fig. 3 B shows recordings from a vomeronasal sensory neuron in which the extracellular addition of 1 mM DIDS produced a block to 42% of its control value. After washout with Ringer's solution, the current amplitude reached 60% of the value before blocker application. On average, the current amplitude in the presence of 1 mM DIDS was 46% ($n = 3$) of the control value (Fig. 3 C). After perfusion with Ringer's solution without DIDS, the current was on average 60% of its control value.

Collectively, these results show that a sudden increase in the intracellular Ca^{2+} concentration can rapidly activate a large anion current, demonstrating the expression of a high density of Ca^{2+}-activated Cl^- channels in the apical region of vomeronasal sensory neurons.

Expression of TMEM16s/anoctamins in mouse VNOs

Having measured Ca^{2+}-activated Cl^- currents in the apical region of mouse vomeronasal sensory neurons, we sought to investigate which members of the TMEM16/anoctamin family that are known to function as Ca^{2+}-activated Cl^- channels are expressed in the VNO.

To analyze the expression of each TMEM16/anoctamin, we performed RT-PCR on cDNA obtained from mouse VNOs. mRNAs of TMEM16A/anoctamin1, B/2, F/6, G/7, J/9, and K/10 were found to be significantly expressed in the VNO (Fig. 4).

Because antibodies against TMEM16A and TMEM16B are commercially available, we first tested their specificity on HEK 293T cells transiently transfected with plasmids containing the cDNA sequence of TMEM16A or TMEM16B and GFP. Fig. 5 shows that cells transfected with TMEM16A (Fig. 5, A–F) or TMEM16B (Fig. 5, G–L)

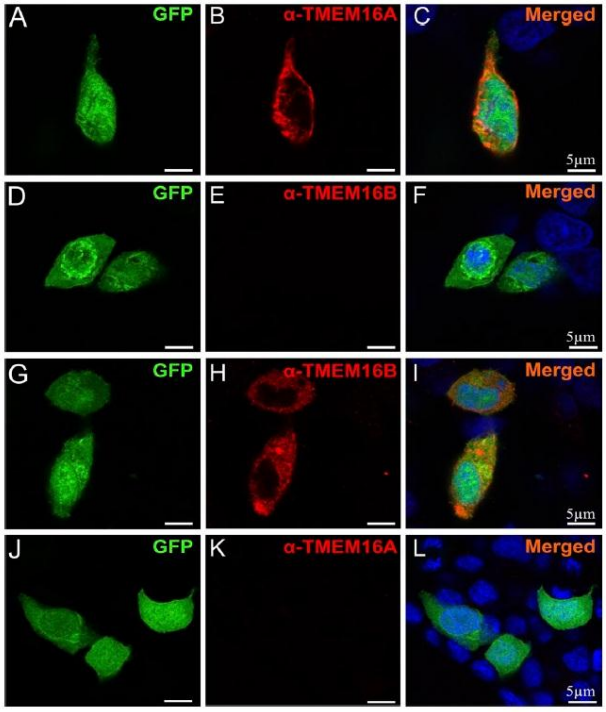

Figure 5. Specificity of rabbit anti-TMEM16A and anti-TMEM16B antibodies in HEK 293T cells expressing TMEM16A or TMEM16B. (A–F) Fluorescence images of the staining with anti-TMEM16A or anti-TMEM16B antibodies (indicated with the prefix α) of HEK 293T cells transiently cotransfected with TMEM16A and GFP cDNA. Specific staining was observed only with anti-TMEM16A (B), whereas no immunoreactivity was detected with anti-TMEM16B (E) antibody. (G–L) Fluorescence images of the staining with anti-TMEM16B or anti-TMEM16A antibodies of HEK 293T cells transiently cotransfected with TMEM16B and GFP cDNA. Specific staining was observed only with anti-TMEM16B (H), whereas no immunoreactivity was detected with anti-TMEM16A (K) antibody. Cell nuclei were stained by DAPI (blue). Bars, 5 μm.

cDNA produced a strong and specific immunoreactivity exclusively to their respective antibody.

We further investigated the specificity of the two antibodies on the olfactory epithelium. Indeed, it is well established that TMEM16B is expressed in the apical layer of the olfactory epithelium but not in the respiratory epithelium (Hengl et al., 2010; Rasche et al., 2010; Billig et al., 2011). We used genetically modified OMP-GFP mice that express GFP in all mature olfactory and vomeronasal sensory neurons (Potter et al., 2001) and confirmed that TMEM16B was expressed at the apical surface of the olfactory epithelium but not in the respiratory epithelium (Fig. 6, D–F), and that TMEM16A immunoreactivity was absent (Fig. 6, A–C). Collectively, these experiments indicate that these antibodies specifically recognized their epitopes and did not show cross-reactivity.

We therefore used the same antibodies to examine the localization of TMEM16A and TMEM16B in the vomeronasal epithelium of OMP-GFP mice and detected immunoreactivity at the luminal surface of the sensory epithelium (Fig. 7, A–F). High magnification images show that both anti-TMEM16A (Fig. 7 G) and anti-TMEM16B (Fig. 7 H) staining lies above the knobs of the vomeronasal sensory neurons, where microvilli are located. We also costained VNO sections with an antibody against the cation channel TRPC2, which is involved in vomeronasal transduction, and observed staining in the microvillar region (Fig. 8, B and E) that largely colocalized with TMEM16A and TMEM16B immunoreactivity (Fig. 8, A, C, D, and F), indicating that cation (TRPC2) and anion channels (TMEM16A and TMEM16B) coexpress. However, the microvillar region is composed of microvilli of both sensory neurons and supporting cells (Höfer et al., 2000; Dauner et al., 2012), and they cannot be distinguished in immunosignals from VNO coronal sections.

To unequivocally establish whether TMEM16A and/or TMEM16B are expressed in the microvilli of sensory neurons, the compartment responsible for signal transduction, we performed immunocytochemistry on isolated vomeronasal sensory neurons using combinations of the commercially available antibodies raised in rabbit and of those raised in guinea pigs (provided by S. Frings; Dauner et al., 2012). Figs. 9 and 10 illustrate that TMEM16A and TMEM16B are both expressed in the microvilli of vomeronasal sensory neurons. Moreover, Fig. 9 clearly shows the coexpression of TMEM16A and TMEM16B in the microvilli of the same neuron from an OMP-GFP mouse. After dissociation and immunocytochemistry procedures, we obtained 34 intact isolated vomeronasal sensory neurons from four OMP-GFP mice, and 62 intact neurons from 10 wild-type mice. Every intact vomeronasal sensory neuron, both from OMP-GFP and wild-type mice, showed coexpression of TMEM16A and TMEM16B in the microvilli. For coexpression, both combinations of rabbit anti-TMEM16A with guinea pig anti-TMEM16B and guinea pig anti-TMEM16A with rabbit anti-TMEM16B produced the same result. Unfortunately, in our preparation of dissociated

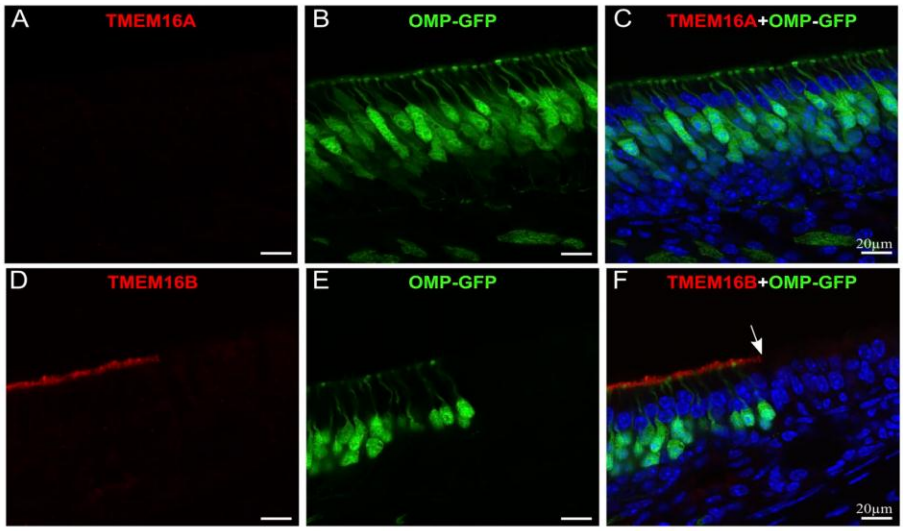

Figure 6. TMEM16A and TMEM16B immunoreactivity in the olfactory epithelium. (A–C) Confocal images of coronal sections of the olfactory epithelium from an OMP-GFP mouse showing the absence of TMEM16A immunoreactivity. (D–F) Confocal images of the transition region between the olfactory and the respiratory epithelium (absence of OMP-GFP–expressing neurons). The arrow indicates the transition between the two epithelia. TMEM16B is expressed at the apical surface of the olfactory but not of the respiratory epithelium. Cell nuclei were stained by DAPI (blue). Bars, 20 µm.

vomeronasal cells, we were not able to clearly identify supporting cells; therefore, we cannot exclude the possibility that TMEM16A and/or TMEM16B are also expressed in microvilli of these cells.

The rodent VNO has two major neuronal populations, apical and basal neurons, characterized by their location in the VNO and by the expression of specific proteins and receptors (Berghard and Buck, 1996; Jia and Halpern, 1996; Ryba and Tirindelli, 1997; Lau and Cherry, 2000; Leinders-Zufall et al., 2004; Liberles et al., 2009; Rivière et al., 2009). Apical neurons are located near the lumen of the VNO and express the G protein α subunit Gαi2, the PDE4A, and receptors of the V1R or formyl peptide receptor family. Basal neurons are close to the basal lamina and express the G protein α subunit Gαo and receptors of the V2R or formyl peptide receptor family. The finding that TMEM16A and TMEM16B are expressed in the microvilli of neurons raises the question of whether the expression of these proteins is restricted to any of these two neuronal subsets. We used specific markers to identify whether neurons expressing TMEM16A or TMEM16B are basal or apical. We performed immunocytochemistry on isolated vomeronasal sensory neurons using rabbit anti-PDE4A antibody, a marker for apical neurons, or rabbit anti-Gαo antibody, a marker for basal neurons (Lau and Cherry, 2000; Leinders-Zufall et al., 2004), together with the guinea pig anti-TMEM16A or anti-TMEM16B. Fig. 10 shows that TMEM16A and TMEM16B are localized in the microvilli of both apical (Fig. 10, A–C and G–I) and basal (Fig. 10, D–F and J–L) vomeronasal sensory neurons from wild-type mice. These results show that TMEM16A and TMEM16B are expressed in microvilli of both the apical and basal neuronal populations.

DISCUSSION

In this study, we have provided the first direct demonstration that a large Cl^- current can be directly activated by Ca^{2+} in the apical region of mouse vomeronasal sensory neurons. Indeed, photolysis of caged Ca^{2+} allowed us to obtain a precise temporal and spatial control of cytoplasmic Ca^{2+} elevation while recording the current in the whole cell voltage-clamp mode. Moreover, we have demonstrated that TMEM16A and TMEM16B largely colocalize with TRPC2 at the apical surface of the vomeronasal epithelium, and that TMEM16A and TMEM16B are coexpressed in microvilli of both apical and basal isolated vomeronasal sensory neurons, therefore suggesting that these two anion channels are likely to be involved in vomeronasal transduction.

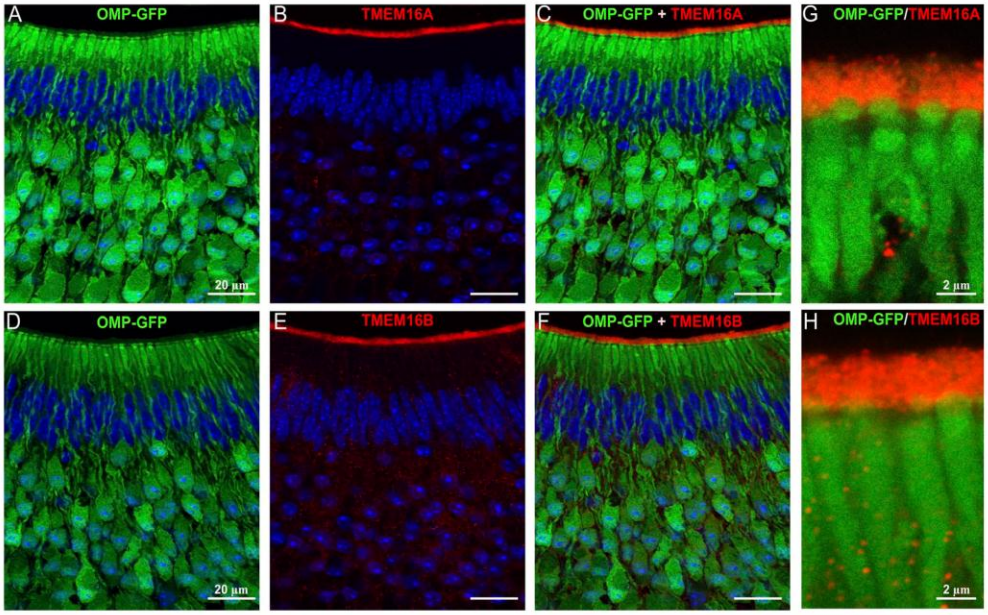

Figure 7. TMEM16A and TMEM16B are expressed at the apical surface of the vomeronasal epithelium. (A–H) Immunostaining of sections of VNO from an OMP-GFP mouse. (A and D) Endogenous GFP fluorescence of mature vomeronasal sensory neurons. TMEM16A (B) and TMEM16B (E) are expressed at the luminal surface of the vomeronasal sensory epithelium. (G and H) High magnification image of the apical portion of the VNO showing that TMEM16A and TMEM16B are expressed at the apical surface. Cell nuclei were stained by DAPI (blue). Bars: (A–F) 20 µm; (G and H) 2 µm.

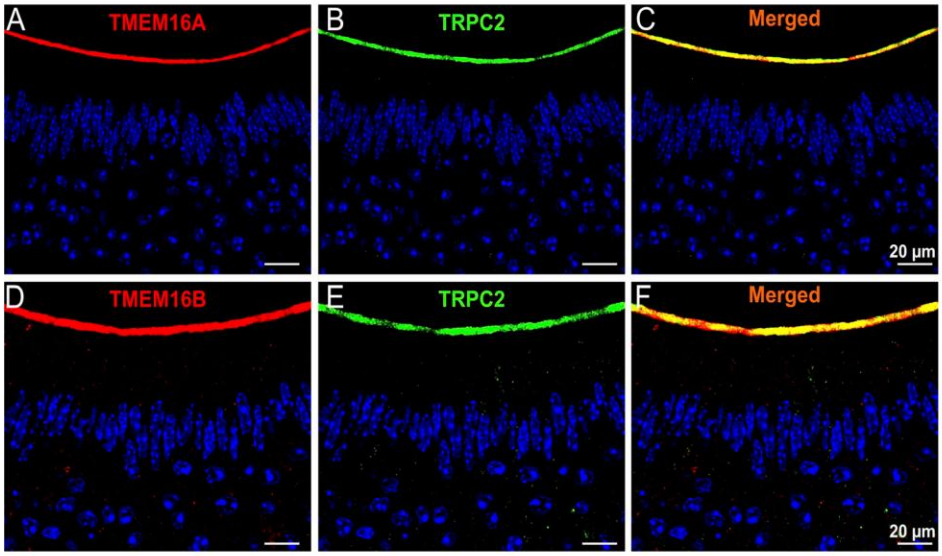

Figure 8. TMEM16A and TMEM16B are coexpressed with TRPC2. Double-label immunohistochemistry in tissue sections of VNO fron a wild-type mouse showing the coexpression of TRPC2 with TMEM16A (A–C) and TMEM16B (D–F) at the luminal surface of the vom eronasal sensory epithelium. Cell nuclei were stained by DAPI (blue). Bars, 20 µm.

Expression of TMEM16A and TMEM16B in the vomeronasal epithelium

Two recent reports (Billig et al., 2011; Dauner et al., 2012) have shown that both TMEM16A and TMEM16B are expressed in the microvillar surface of the VNO. However, as pointed out by Dauner et al. (2012), the VNO apical surface layer contains the microvilli of both sensory neurons and supporting cells (Höfer et al., 2000). Thus, immunohistochemistry on coronal sections of the VNO does not allow for the distinction between these two microvillar subsets. By performing high reso lution confocal imaging on isolated vomeronasal sen sory neurons, we were able to detect both TMEM16A and TMEM16B in microvilli of the same neuron, thu providing the first unequivocal evidence of coexpres sion of these two anion channels in the same cell.

Ca^{2+}-activated currents in vomeronasal sensory neurons

Previous reports showed the presence of Ca^{2+}-activated nonselective cation currents in vomeronasal sensor

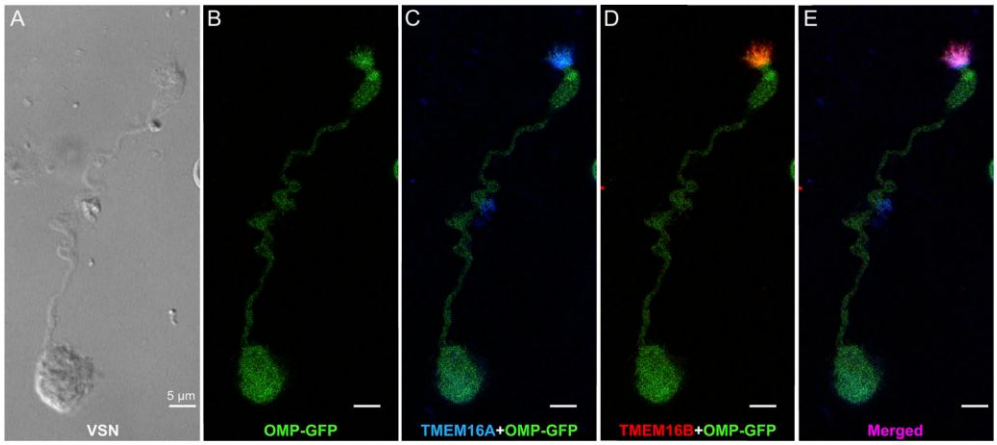

Figure 9. TMEM16A and TMEM16B are coexpressed in the microvilli of vomeronasal sensory neurons. (A) Bright field image of vomeronasal sensory neuron isolated from an OMP-GFP mouse (B). The same neuron was stained with (C) rabbit anti-TMEM16A and (D) guinea pig anti-TMEM16B, showing the coexpression of the two anion channels in the microvilli (E). Cell nuclei were stained b DAPI (blue). Bars, 5 µm.

neurons (Liman, 2003; Spehr et al., 2009). In our experiments, with intracellular Cs^+ and extracellular Na^+ as the main monovalent cations, we did not detect any cation current. However, it must be pointed out that the anion and cation channels are likely to be activated in two very different ranges of Ca^{2+} concentration. Liman (2003) reported that half-activation of the nonselective cation channel occurred at a very high Ca^{2+} concentration: 0.5 mM at −80 mV. The Ca^{2+}-activated Cl^- channels TMEM16A and TMEM16B, located in the microvilli of vomeronasal sensory neurons, are half-activated at <5 µM (Pifferi et al., 2009a; Stephan et al., 2009; Xiao et al., 2011), a Ca^{2+} concentration that is 100-fold lower than that required to activate the nonselective cation currents. Moreover, although we did not directly measure the Ca^{2+} concentration photoreleased in the microvilli, estimates from our previous studies in olfactory sensory neurons obtained by comparing the normalized currents at various flash intensities (Boccaccio et al., 2006) with the dose–response relation for the native olfactory Ca^{2+}-activated Cl^- channels (Pifferi et al., 2009b) indicate that the maximal photoreleased concentration of Ca^{2+} is likely to be ∼10–20 µM. Thus, a Ca^{2+} concentration range lower than that necessary to activate the nonselective cation channels may explain the lack of detectable cation currents in our experiments.

Liman (2003) also stimulated inside-out patches from dendritic knobs of hamster vomeronasal sensory neurons with 2 mM Ca^{2+} and showed that the activated current was almost entirely cationic. Similar results were obtained by Spehr et al. (2009) by activating patches from mouse VNO neurons with 50 µM Ca^{2+}. It is likely that the explanation of the absence of the chloride component in these inside-out experiments is related to a rapid decrease of the current. Indeed, it has been shown that Ca^{2+}-activated Cl^- channels have a fast rundown in activity after patch excision from the dendritic knob of rat olfactory sensory neurons (Reisert et al., 2003) and that a detectable chloride current is present only in 75% of the patches from mouse olfactory sensory neurons (Fig. 6 C of Pifferi et al., 2009b).

A few recent studies have also provided some evidence for the presence of Ca^{2+}-activated Cl^- channels in vomeronasal sensory neurons. Yang and Delay (2010) used the perforated patch-clamp recordings with gramicidin, a technique that does not modify the intracellular Cl^- concentration, and demonstrated that 80% of the urine-induced current was carried by Ca^{2+}-activated Cl^- channels. These authors also showed that Ca^{2+} influx is

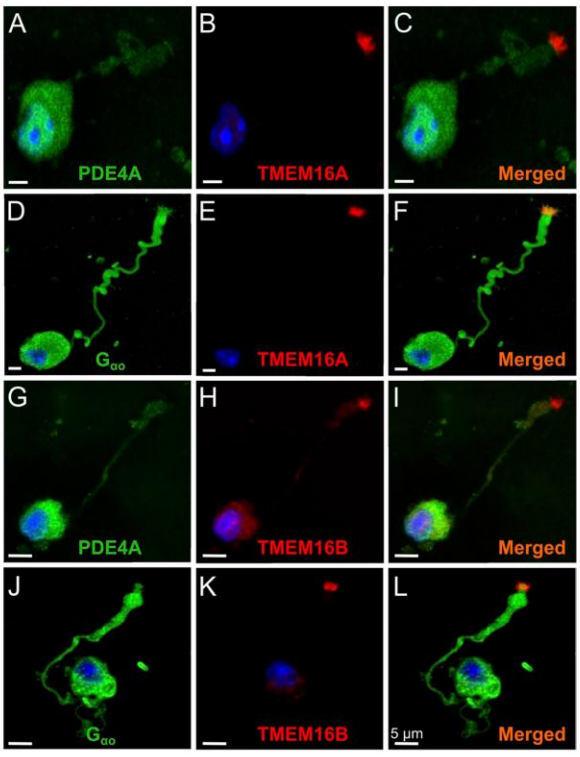

Figure 10. TMEM16A and TMEM16B are expressed in the microvilli of both apical and basal vomeronasal sensory neurons. TMEM16A (guinea pig antibody) is expressed in the microvilli of both apical neurons, as shown by PDE4A (A–C) immunoreactivity, and basal neurons, labeled with rabbit anti-Gαo antibody (D–F). TMEM16B (guinea pig antibody) is also located in the microvilli of both apical (G–I) and basal (J–L) neurons. Cell nuclei were stained by DAPI (blue). Bars, 5 µm.

necessary to activate the Cl^- channels. In another study, Kim et al. (2011) confirmed the previous study of Yang and Delay (2010) showing that a Ca^{2+}-activated Cl^- current contributes to urine response, but they also suggested that this current can be activated both by Ca^{2+} influx through the TRPC2 channel and by Ca^{2+} release from intracellular stores. Indeed, they also showed that knockout mice for TRPC2 still have a Ca^{2+}-activated Cl^- component in the response to urine that is blocked by compounds that inhibit intracellular Ca^{2+} release, thus suggesting that a TRPC2-independent signaling pathway may be operating in the VNO and that the Ca^{2+}-activated Cl^- current may play a relevant role in transduction.

Billig et al. (2011) compared whole cell recordings in vomeronasal sensory neurons from wild-type ($n = 7$) or knockout mice for TMEM16B ($Ano2^{-/-}$; $n = 6$) obtained with 1.5 µM Ca^{2+} or 0 Ca^{2+} in the pipette and reported that "currents of most $Ano2^{-/-}$ VSNs were indistinguishable from those we observed without Ca^{2+} (Fig. 5n), but a few cells showed currents up to twofold larger. Averaged current/voltage curves revealed that Ca^{2+}-activated Cl^- currents of VSNs depend predominantly on Ano2 (Fig. 5l). Although Ano1 is expressed in the VNO (Fig. 3a), its contribution to VSN currents seems minor." Thus, although most of the Ca^{2+}-activated current was abolished in knockout mice for TMEM16B, a residual current was still present in some neurons. It is likely that the residual current is carried by TMEM16A channels. Indeed, both TMEM16A and TMEM16B are known to independently function as Ca^{2+}-activated Cl^- channels (Scudieri et al., 2012), and we have demonstrated that TMEM16A and TMEM16B coexpress in microvilli of vomeronasal sensory neurons. Further experiments are necessary to unequivocally establish the origin of the residual current and to determine whether TMEM16A and TMEM16B form heteromeric channels and, if so, what the functional properties of the heteromeric channels are.

Physiological role of Ca^{2+}-activated Cl^- channels in vomeronasal and olfactory transduction

What is, then, the physiological role of Ca^{2+}-activated Cl^- channels in vomeronasal sensory neurons? Depending on the Cl^- equilibrium potential, these channels may contribute to the neuron depolarization or hyperpolarization. In vomeronasal sensory neurons, estimates of the Cl^- concentration inside the neurons and in the fluid filling its lumen are not available yet. However, experiments with the perforated patch-clamp recordings with gramicidin showed that the Ca^{2+}-activated Cl^- current acts to further amplify a primary inward depolarizing current (Yang and Delay, 2010), indicating that the intracellular Cl^- concentration was relatively high. In addition, the same authors showed that bumetanide, a specific blocker for the sodium potassium–chloride cotransporter NKCC1, significantly decreased the urine-induced inward current, indicating that NKCC1 is involved in chloride accumulation.

In olfactory sensory neurons, direct measurements of Cl^- concentrations showed that these neurons maintain an unusually high internal concentration of Cl^- of ~50 mM, which is similar to the Cl^- concentration present in the mucus at the external side of the ciliary membrane (Reuter et al., 1998; Kaneko et al., 2001, 2004). Therefore, in physiological conditions, the opening of Ca^{2+}-activated Cl^- channels causes an efflux of Cl^- ions from the cilia, which contributes to neuron depolarization. Up to 80% of the transduction current can be carried by Cl^-. Furthermore, studies from several laboratories indicated that TMEM16B is the main constituent of the Ca^{2+}-activated Cl^- channels involved in olfactory transduction. Indeed, it has been shown that TMEM16B is expressed in the ciliary layer of the olfactory epithelium, that currents in olfactory sensory neurons and in HEK 293T cells transfected with TMEM16B have very similar characteristics, and that knockout mice for TMEM16B did not show any detectable Ca^{2+}-activated Cl^- current (Pifferi et al., 2012). However, Billig et al. (2011) found that disruption of TMEM16B did not reduce mouse performance in some classical olfactory behavioral tasks, suggesting that Ca^{2+}-activated Cl^- channels may be dispensable for near-normal olfaction. Future experiments will have to establish whether Ca^{2+}-activated Cl^- channels are involved in more subtle aspects of olfactory sensing not detected in previous experiments.

It is of interest to note that, despite their differences in the molecular mechanisms of transduction, both olfactory and vomeronasal neurons express members of the TMEM16 family at the site of transduction, indicating that these channels are likely to play a physiological role in sensory transduction.

Conclusions

Our data contribute to the present understanding of the molecular mechanisms of vomeronasal transduction by providing the first direct evidence of the presence of a large Ca^{2+}-activated Cl^- current in the apical region of mouse vomeronasal sensory neurons and of the coexpression of the two Ca^{2+}-activated Cl^- channels TMEM16A and TMEM16B in the microvilli of the same sensory neurons. These observations suggest that TMEM16A and TMEM16B are likely to be responsible for the Cl^- current reported in this work.

In conclusion, collectively with previous studies indicating the presence of a Ca^{2+}-activated Cl^- component in urine response (Yang and Delay, 2010; Kim et al., 2011), our results contribute to the indication that Ca^{2+}-activated Cl^- channels could play a role in vomeronasal transduction. Future studies in mice in which the TMEM16A and/or TMEM16B gene are deleted will increase our understanding of the role of intracellular Ca^{2+} elevation in vomeronasal transduction.

We thank Stephan Frings (Heidelberg University, Heidelberg, Germany) for providing guinea pig antibodies against TMEM16A and TMEM16B, Peter Mombaerts (Max Planck Institute of Biophysics, Frankfurt, Germany) for providing OMP-GFP mice, Johannes Reisert for helpful discussions, Simone Pifferi and Anna Boccaccio for comments on the manuscript, and all members of the laboratories for discussions.

This study was supported by grants from the Italian Ministry of Education, University and Research, and from the Italian Institute of Technology.

Edward N. Pugh Jr. served as editor.

Submitted: 2 February 2012
Accepted: 6 June 2012

REFERENCES

Arnson, H.A., X. Fu, and T.E. Holy. 2010. Multielectrode array recordings of the vomeronasal epithelium. *J. Vis. Exp.* 1845.

Barry, P.H. 1994. JPCalc, a software package for calculating liquid junction potential corrections in patch-clamp, intracellular, epithelial and bilayer measurements and for correcting junction potential measurements. *J. Neurosci. Methods.* 51:107–116. http://dx.doi.org/10.1016/0165-0270(94)90031-0

Berghard, A., and L.B. Buck. 1996. Sensory transduction in vomeronasal neurons: evidence for G alpha o, G alpha i2, and adenylyl cyclase II as major components of a pheromone signaling cascade. *J. Neurosci.* 16:909–918.

Billig, G.M., B. Pál, P. Fidzinski, and T.J. Jentsch. 2011. Ca^{2+}-activated Cl^- currents are dispensable for olfaction. *Nat. Neurosci.* 14:763–769. http://dx.doi.org/10.1038/nn.2821

Boccaccio, A., and A. Menini. 2007. Temporal development of cyclic nucleotide-gated and Ca^{2+} -activated Cl^- currents in isolated mouse olfactory sensory neurons. *J. Neurophysiol.* 98:153–160. http://dx.doi.org/10.1152/jn.00270.2007

Boccaccio, A., L. Lagostena, V. Hagen, and A. Menini. 2006. Fast adaptation in mouse olfactory sensory neurons does not require the activity of phosphodiesterase. *J. Gen. Physiol.* 128:171–184. http://dx.doi.org/10.1085/jgp.200609555

Boccaccio, A., C. Sagheddu, and A. Menini. 2011. Flash photolysis of caged compounds in the cilia of olfactory sensory neurons. *J. Vis. Exp.* e3195.

Brennan, P.A. 2009. Pheromones and mammalian behavior. *In* The Neurobiology of Olfaction. A. Menini, editor. CRC Press, Boca Raton, FL. 157–179.

Brennan, P.A., and F. Zufall. 2006. Pheromonal communication in vertebrates. *Nature.* 444:308–315. http://dx.doi.org/10.1038/nature05404

Caputo, A., E. Caci, L. Ferrera, N. Pedemonte, C. Barsanti, E. Sondo, U. Pfeffer, R. Ravazzolo, O. Zegarra-Moran, and L.J.V. Galietta. 2008. TMEM16A, a membrane protein associated with calcium-dependent chloride channel activity. *Science.* 322:590–594. http://dx.doi.org/10.1126/science.1163518

Chamero, P., T.F. Marton, D.W. Logan, K. Flanagan, J.R. Cruz, A. Saghatelian, B.F. Cravatt, and L. Stowers. 2007. Identification of protein pheromones that promote aggressive behaviour. *Nature.* 450:899–902. http://dx.doi.org/10.1038/nature05997

Dauner, K., J. Lissmann, S. Jeridi, S. Frings, and F. Möhrlen. 2012. Expression patterns of anoctamin 1 and anoctamin 2 chloride channels in the mammalian nose. *Cell Tissue Res.* 347:327–341. http://dx.doi.org/10.1007/s00441-012-1324-9

Dean, D.M., A. Mazzatenta, and A. Menini. 2004. Voltage-activated current properties of male and female mouse vomeronasal sensory neurons: sexually dichotomous? *J. Comp. Physiol. A Neuroethol. Sens. Neural Behav. Physiol.* 190:491–499. http://dx.doi.org/10.1007/s00359-004-0513-8

Dibattista, M., A. Mazzatenta, F. Grassi, R. Tirindelli, and A. Menini. 2008. Hyperpolarization-activated cyclic nucleotide-gated channels in mouse vomeronasal sensory neurons. *J. Neurophysiol.* 100:576–586. http://dx.doi.org/10.1152/jn.90263.2008

Fieni, F., V. Ghiaroni, R. Tirindelli, P. Pietra, and A. Bigiani. 2003. Apical and basal neurones isolated from the mouse vomeronasal organ differ for voltage-dependent currents. *J. Physiol.* 552:425–436. http://dx.doi.org/10.1113/jphysiol.2003.052035

Frings, S. 2009a. Chloride-based signal amplification in olfactory sensory neurons. *In* Physiology and Pathology of Chloride Transporters and Channels in the Nervous System. From Molecules to Diseases. F. J. Alvarez-Leefmans and E. Delpire, editors. Elsevier-Academic Press, San Diego, CA. 413–424.

Frings, S. 2009b. Primary processes in sensory cells: current advances. *J. Comp. Physiol. A Neuroethol. Sens. Neural Behav. Physiol.* 195:1–19. http://dx.doi.org/10.1007/s00359-008-0389-0

Frings, S., D. Reuter, and S.J. Kleene. 2000. Neuronal Ca^{2+}-activated Cl^- channels—homing in on an elusive channel species. *Prog. Neurobiol.* 60:247–289. http://dx.doi.org/10.1016/S0301-0082(99)00027-1

Hartzell, C., I. Putzier, and J. Arreola. 2005. Calcium-activated chloride channels. *Annu. Rev. Physiol.* 67:719–758. http://dx.doi.org/10.1146/annurev.physiol.67.032003.154341

Hengl, T., H. Kaneko, K. Dauner, K. Vocke, S. Frings, and F. Möhrlen. 2010. Molecular components of signal amplification in olfactory sensory cilia. *Proc. Natl. Acad. Sci. USA.* 107:6052–6057. http://dx.doi.org/10.1073/pnas.0909032107

Höfer, D., D.W. Shin, and D. Drenckhahn. 2000. Identification of cytoskeletal markers for the different microvilli and cell types of the rat vomeronasal sensory epithelium. *J. Neurocytol.* 29:147–156. http://dx.doi.org/10.1023/A:1026548020851

Holy, T.E., C. Dulac, and M. Meister. 2000. Responses of vomeronasal neurons to natural stimuli. *Science.* 289:1569–1572. http://dx.doi.org/10.1126/science.289.5484.1569

Jia, C., and M. Halpern. 1996. Subclasses of vomeronasal receptor neurons: differential expression of G proteins (Gi alpha 2 and G(o alpha)) and segregated projections to the accessory olfactory bulb. *Brain Res.* 719:117–128. http://dx.doi.org/10.1016/0006-8993(96)00110-2

Kaneko, H., T. Nakamura, and B. Lindemann. 2001. Noninvasive measurement of chloride concentration in rat olfactory receptor cells with use of a fluorescent dye. *Am. J. Physiol. Cell Physiol.* 280:C1387–C1393.

Kaneko, H., I. Putzier, S. Frings, U.B. Kaupp, and T. Gensch. 2004. Chloride accumulation in mammalian olfactory sensory neurons. *J. Neurosci.* 24:7931–7938. http://dx.doi.org/10.1523/JNEUROSCI.2115-04.2004

Kim, S., L. Ma, and C.R. Yu. 2011. Requirement of calcium-activated chloride channels in the activation of mouse vomeronasal neurons. *Nat Commun.* 2:365. http://dx.doi.org/10.1038/ncomms1368

Kleene, S.J. 2008. The electrochemical basis of odor transduction in vertebrate olfactory cilia. *Chem. Senses.* 33:839–859. http://dx.doi.org/10.1093/chemse/bjn048

Lau, Y.E., and J.A. Cherry. 2000. Distribution of PDE4A and G(o) alpha immunoreactivity in the accessory olfactory system of the mouse. *Neuroreport.* 11:27–32. http://dx.doi.org/10.1097/00001756-200001170-00006

Leinders-Zufall, T., A.P. Lane, A.C. Puche, W. Ma, M.V. Novotny, M.T. Shipley, and F. Zufall. 2000. Ultrasensitive pheromone detection by mammalian vomeronasal neurons. *Nature.* 405:792–796. http://dx.doi.org/10.1038/35015572

Leinders-Zufall, T., P. Brennan, P. Widmayer, P.C. S, A. Maul-Pavicic, M. Jäger, X.H. Li, H. Breer, F. Zufall, and T. Boehm. 2004. MHC class I peptides as chemosensory signals in the vomeronasal organ. *Science.* 306:1033–1037. http://dx.doi.org/10.1126/science.1102818

Leinders-Zufall, T., T. Ishii, P. Mombaerts, F. Zufall, and T. Boehm. 2009. Structural requirements for the activation of vomeronasal sensory neurons by MHC peptides. *Nat. Neurosci.* 12:1551–1558. http://dx.doi.org/10.1038/nn.2452

Liberles, S.D., L.F. Horowitz, D. Kuang, J.J. Contos, K.L. Wilson, J. Siltberg-Liberles, D.A. Liberles, and L.B. Buck. 2009. Formyl peptide receptors are candidate chemosensory receptors in the vomeronasal organ. *Proc. Natl. Acad. Sci. USA.* 106:9842–9847. http://dx.doi.org/10.1073/pnas.0904464106

Liman, E.R. 2003. Regulation by voltage and adenine nucleotides of a Ca^{2+}-activated cation channel from hamster vomeronasal sensory neurons. *J. Physiol.* 548:777–787. http://dx.doi.org/10.1113/jphysiol.2002.037119

Liman, E.R., and D.P. Corey. 1996. Electrophysiological characterization of chemosensory neurons from the mouse vomeronasal organ. *J. Neurosci.* 16:4625–4637.

Liman, E.R., D.P. Corey, and C. Dulac. 1999. TRP2: a candidate transduction channel for mammalian pheromone sensory signaling. *Proc. Natl. Acad. Sci. USA.* 96:5791–5796. http://dx.doi.org/10.1073/pnas.96.10.5791

Ma, M. 2009. Multiple olfactory subsystems convey various sensory signals. *In* The Neurobiology of Olfaction. A. Menini, editor. CRC Press, Boca Raton, FL. 225–240.

Munger, S.D., T. Leinders-Zufall, and F. Zufall. 2009. Subsystem organization of the mammalian sense of smell. *Annu. Rev. Physiol.* 71:115–140. http://dx.doi.org/10.1146/annurev.physiol.70.113006.100608

Pifferi, S., A. Boccaccio, and A. Menini. 2006. Cyclic nucleotide-gated ion channels in sensory transduction. *FEBS Lett.* 580:2853–2859. http://dx.doi.org/10.1016/j.febslet.2006.03.086

Pifferi, S., M. Dibattista, and A. Menini. 2009a. TMEM16B induces chloride currents activated by calcium in mammalian cells. *Pflugers Arch.* 458:1023–1038. http://dx.doi.org/10.1007/s00424-009-0684-9

Pifferi, S., M. Dibattista, C. Sagheddu, A. Boccaccio, A. Al Qteishat, F. Ghirardi, R. Tirindelli, and A. Menini. 2009b. Calcium-activated chloride currents in olfactory sensory neurons from mice lacking bestrophin-2. *J. Physiol.* 587:4265–4279. http://dx.doi.org/10.1113/jphysiol.2009.176131

Pifferi, S., V. Cenedese, and A. Menini. 2012. Anoctamin 2/TMEM16B: a calcium-activated chloride channel in olfactory transduction. *Exp. Physiol.* 97:193–199.

Potter, S.M., C. Zheng, D.S. Koos, P. Feinstein, S.E. Fraser, and P. Mombaerts. 2001. Structure and emergence of specific olfactory glomeruli in the mouse. *J. Neurosci.* 21:9713–9723.

Rasche, S., B. Toetter, J. Adler, A. Tschapek, J.F. Doerner, S. Kurtenbach, H. Hatt, H. Meyer, B. Warscheid, and E.M. Neuhaus. 2010. Tmem16b is specifically expressed in the cilia of olfactory sensory neurons. *Chem. Senses.* 35:239–245. http://dx.doi.org/10.1093/chemse/bjq007

Reisert, J., and H. Zhao. 2011. Perspectives on: Information and coding in mammalian sensory physiology: Response kinetics of olfactory receptor neurons and the implications in olfactory coding. *J. Gen. Physiol.* 138:303–310. http://dx.doi.org/10.1085/jgp.201110645

Reisert, J., P.J. Bauer, K.W. Yau, and S. Frings. 2003. The Ca-activated Cl channel and its control in rat olfactory receptor neurons. *J. Gen. Physiol.* 122:349–363. http://dx.doi.org/10.1085/jgp.200308888

Reuter, D., K. Zierold, W.H. Schröder, and S. Frings. 1998. A depolarizing chloride current contributes to chemoelectrical transduction in olfactory sensory neurons in situ. *J. Neurosci.* 18:6623–6630.

Rivière, S., L. Challet, D. Fluegge, M. Spehr, and I. Rodriguez. 2009. Formyl peptide receptor-like proteins are a novel family of vomeronasal chemosensors. *Nature.* 459:574–577. http://dx.doi.org/10.1038/nature08029

Ryba, N.J., and R. Tirindelli. 1997. A new multigene family of putative pheromone receptors. *Neuron.* 19:371–379. http://dx.doi.org/10.1016/S0896-6273(00)80946-0

Sagheddu, C., A. Boccaccio, M. Dibattista, G. Montani, R. Tirindelli, and A. Menini. 2010. Calcium concentration jumps reveal dynamic ion selectivity of calcium-activated chloride currents in mouse olfactory sensory neurons and TMEM16b-transfected HEK 293T cells. *J. Physiol.* 588:4189–4204. http://dx.doi.org/10.1113/jphysiol.2010.194407

Schild, D., and D. Restrepo. 1998. Transduction mechanisms in vertebrate olfactory receptor cells. *Physiol. Rev.* 78:429–466.

Schroeder, B.C., T. Cheng, Y.N. Jan, and L.Y. Jan. 2008. Expression cloning of TMEM16A as a calcium-activated chloride channel subunit. *Cell.* 134:1019–1029. http://dx.doi.org/10.1016/j.cell.2008.09.003

Scudieri, P., E. Sondo, L. Ferrera, and L.J. Galietta. 2012. The anoctamin family: TMEM16A and TMEM16B as calcium-activated chloride channels. *Exp. Physiol.* 97:177–183. http://dx.doi.org/10.1113/expphysiol.2011.058198

Shimazaki, R., A. Boccaccio, A. Mazzatenta, G. Pinato, M. Migliore, and A. Menini. 2006. Electrophysiological properties and modeling of murine vomeronasal sensory neurons in acute slice preparations. *Chem. Senses.* 31:425–435. http://dx.doi.org/10.1093/chemse/bjj047

Spehr, M., H. Hatt, and C.H. Wetzel. 2002. Arachidonic acid plays a role in rat vomeronasal signal transduction. *J. Neurosci.* 22:8429–8437.

Spehr, J., S. Hagendorf, J. Weiss, M. Spehr, T. Leinders-Zufall, and F. Zufall. 2009. Ca^{2+}-calmodulin feedback mediates sensory adaptation and inhibits pheromone-sensitive ion channels in the vomeronasal organ. *J. Neurosci.* 29:2125–2135. http://dx.doi.org/10.1523/JNEUROSCI.5416-08.2009

Stephan, A.B., E.Y. Shum, S. Hirsh, K.D. Cygnar, J. Reisert, and H. Zhao. 2009. ANO2 is the cilial calcium-activated chloride channel that may mediate olfactory amplification. *Proc. Natl. Acad. Sci. USA.* 106:11776–11781. http://dx.doi.org/10.1073/pnas.0903304106

Stöhr, H., J.B. Heisig, P.M. Benz, S. Schöberl, V.M. Milenkovic, O. Strauss, W.M. Aartsen, J. Wijnholds, B.H.F. Weber, and H.L. Schulz. 2009. TMEM16B, a novel protein with calcium-dependent chloride channel activity, associates with a presynaptic protein complex in photoreceptor terminals. *J. Neurosci.* 29:6809–6818. http://dx.doi.org/10.1523/JNEUROSCI.5546-08.2009

Tirindelli, R., M. Dibattista, S. Pifferi, and A. Menini. 2009. From pheromones to behavior. *Physiol. Rev.* 89:921–956. http://dx.doi.org/10.1152/physrev.00037.2008

Touhara, K., and L.B. Vosshall. 2009. Sensing odorants and pheromones with chemosensory receptors. *Annu. Rev. Physiol.* 71:307–332. http://dx.doi.org/10.1146/annurev.physiol.010908.163209

Xiao, Q., K. Yu, P. Perez-Cornejo, Y. Cui, J. Arreola, and H.C. Hartzell. 2011. Voltage- and calcium-dependent gating of TMEM16A/Ano1 chloride channels are physically coupled by the first intracellular loop. *Proc. Natl. Acad. Sci. USA.* 108:8891–8896. http://dx.doi.org/10.1073/pnas.1102147108

Yang, C., and R.J. Delay. 2010. Calcium-activated chloride current amplifies the response to urine in mouse vomeronasal sensory neurons. *J. Gen. Physiol.* 135:3–13. http://dx.doi.org/10.1085/jgp.200910265

Yang, Y.D., H. Cho, J.Y. Koo, M.H. Tak, Y. Cho, W.-S. Shim, S.P. Park, J. Lee, B. Lee, B.-M. Kim, et al. 2008. TMEM16A confers receptor-activated calcium-dependent chloride conductance. *Nature.* 455:1210–1215. http://dx.doi.org/10.1038/nature07313

Zufall, F., K. Ukhanov, P. Lucas, E.R. Liman, and T. Leinders-Zufall. 2005. Neurobiology of TRPC2: from gene to behavior. *Pflugers Arch.* 451:61–71.

Zufall, F., and T. Leinders-Zufall. 2007. Mammalian pheromone sensing. *Curr. Opin. Neurobiol.* 17:483–489. http://dx.doi.org/10.1016/j.conb.2007.07.012

2. **Characterization of Ca^{2+}-activated chloride current in isolated mouse vomeronasal sensory neurons**

   Amjad A, Pifferi S, Boccaccio A, Menini A

   Manuscript in preparation

Properties of native Ca^{2+}-activated currents at different levels of $[Ca^{2+}]_i$.

Ca^{2+}-activated currents in VSNs

Our previous work has shown that CaCCs are present in the apical region of mouse VSNs (Dibattista *et al.,* 2012). Indeed, intracellular calcium jump upon photorelease of caged Ca^{2+} fast activated a chloride-mediated current. Here, we recorded the Ca^{2+}-activated currents in VSNs using the whole-cell configuration of the patch-clamp technique dialyzing the cells with intracellular solutions with different free Ca^{2+} concentrations. **Fig.1 A and B** shows that voltage steps between -100 mV and +100 mV, from a holding potential of 0 mV, with $[Ca^{2+}]_i$<10 nM, induced negligible currents compared to those measured in the presence of higher $[Ca^{2+}]_i$. The dialysis of VSNs with intracellular solution with $[Ca^{2+}]_i$ in the micromolar range induced robust currents with an average of 1.5 nA at +100 mV(range 0.6-3.7 nA, n=12). Increasing $[Ca^{2+}]_i$ to 2mM did not further significantly increased the amplitude of the current. Upon depolarization, Ca^{2+}-activated currents showed instantaneous activation followed by a time dependent outward relaxation, while hyperpolarizing voltage steps induced instantaneous inward currents followed by a relaxation toward less negative values.

To study the Ca^{2+}dependence of the current we measured the instantaneous tail currents at −100 mV after voltage steps from +100 and -100 mV. Tail current amplitudes versus $[Ca^{2+}]_i$ were plotted in **Fig.1 C** and fitted with the Hill equation:

$$\frac{I}{I_{max}} = \frac{[Ca^{2+}]^{n_H}}{[Ca^{2+}]^{n_H} + K_{1/2}^{n_H}}$$

Where I_{max} is the average of the tail current measured at -100 mV from a step of +100mV in the presence of 2 mM $[Ca^{2+}]_i$, $K_{1/2}$ is the $[Ca^{2+}]_i$ concentration producing 50% of I_{max} and n_H is the Hill coefficient. $K_{1/2}$ decreased with membrane depolarization from about 1.4 µM at -100mV to 0.6 µM at +100mV (**Fig.1 D**).

The kinetics of voltage-dependent relaxation was well fitted with a monoexponential function and depended on $[Ca^{2+}]_i$. Indeed, the time constant of

activation at +100mV was 206 ± 17 ms with 0.5 µM $[Ca^{2+}]_i$ and 69 ± 7 ms with 2 mM. Similarly the time constant of deactivation at -100mV was 46 ± 8 ms with 0.5 µM $[Ca^{2+}]_i$ and 18 ± 2 ms with 2 mM$[Ca^{2+}]_i$ (**Fig.1 E-F)**.

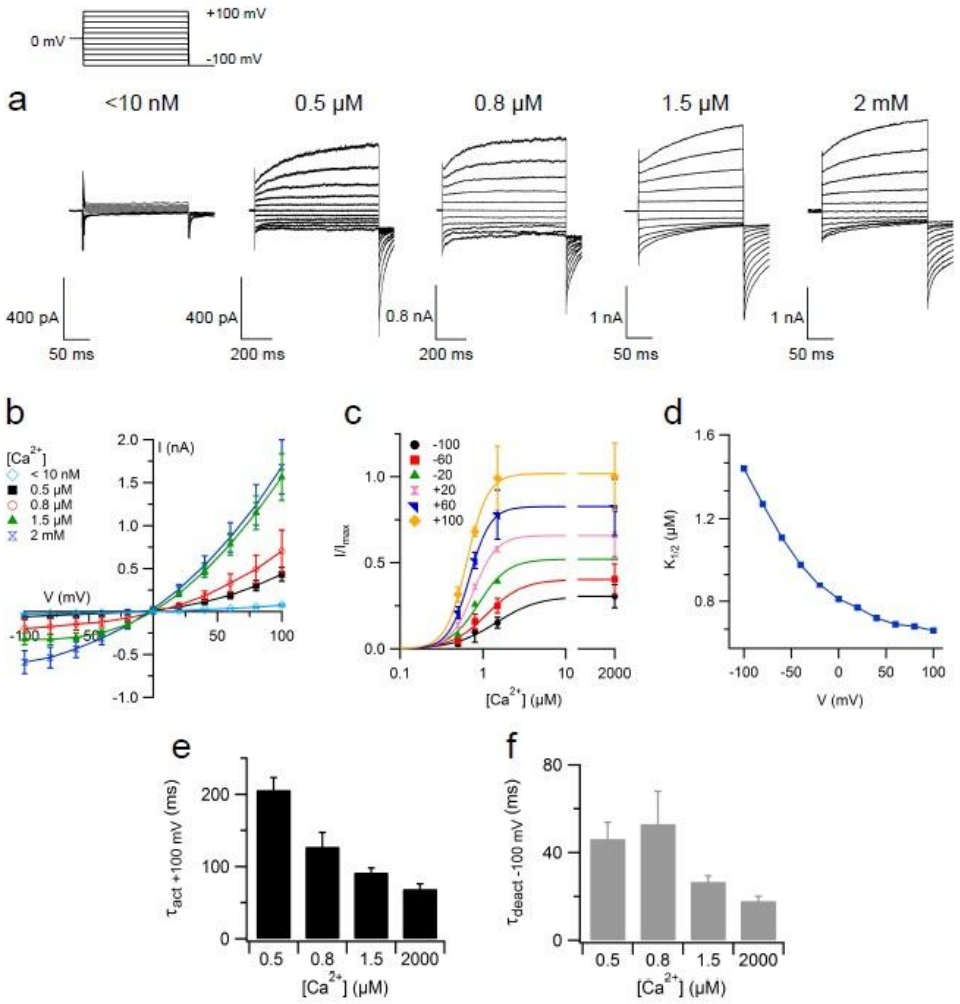

Fig 1: Voltage-dependent Ca^{2+}-activated currents in mouse VSNs. **(A)** Whole cell currents recorded from different neurons at the indicated levels of $[Ca^{2+}]_i$ during voltage steps of 200ms duration from a holding potential of 0mV to voltages between -100 and +100 mV in 20mV steps followed by a step to -100mV. Step duration was 200 ms in low Ca^{2+}, 1.5 µM and 2 mM, while longer duration of 500 ms was used for 0.5 and 0.8 µM, because the activation kinetics was slower. **(B)** Steady-state current voltage relationship from several cells (n = 3-12). **(C)** Normalized tail currents at −100 mV voltage steps plotted vs. free $[Ca^{2+}]_i$ and fitted to the Hill equation. **(D)** $K_{1/2}$ values plotted versus voltage. **(E)** Average activation and **(F)** deactivation kinetics of Ca^{2+} activated currents were evaluated with an exponential fit respectively at $\pm$100mV. Mean values $\pm$ SEM were plotted versus indicated $[Ca^{2+}]i$.

Voltage-dependence of Ca^{2+}-activated currents in VSNs

To check if the outward rectification of Ca^{2+}-activated currents measured at the steady-state is an intrinsic property of the open channel or it is due to voltage-dependence of the open probability, we performed a prepulse protocol as shown in **Fig.2 A**. Current were activated at +100 mV for 100ms and then the voltage was stepped between -60 and +60 with 20 mV of increment. Both instantaneous and steady-state currents were measured and plotted in **Fig.2 B**. While the steady-state current showed an outward rectification the instantaneous current had a linear IV-relationship, demonstrating that the outward rectification is a result of a voltage-dependent mechanism that favors channel opening at depolarizing voltages.

The voltage-dependence of the steady-state activation was analyzed by plotting the steady-state conductance versus voltage at various $[Ca^{2+}]_i$ in **Fig.2 C** and fitted with the Boltzmann equation:

$$\frac{G}{Gmax} = 1/\{1 + \exp[z(V\frac{1}{2} - V)\ F\ /RT]\}$$

Where G/Gmax is the normalized conductance, z is the equivalent gating charge associated with voltage-dependent channel opening, V is the membrane potential, $V_{1/2}$ is the membrane potential producing half-maximal activation, F is the Faraday constant, R is the gas constant, and T is the absolute temperature.$V_{1/2}$ was 212 mV at 0.5µM Ca^{2+} and decreased to -4 mV at 2 mM Ca^{2+} **(Fig.2 D)**. The decrease of $V_{1/2}$ as $[Ca^{2+}]_i$ increased indicates that more channels can be activated by depolarization at higher $[Ca^{2+}]_i$ showing that the conductance depends both on $[Ca^{2+}]_i$ and voltage.

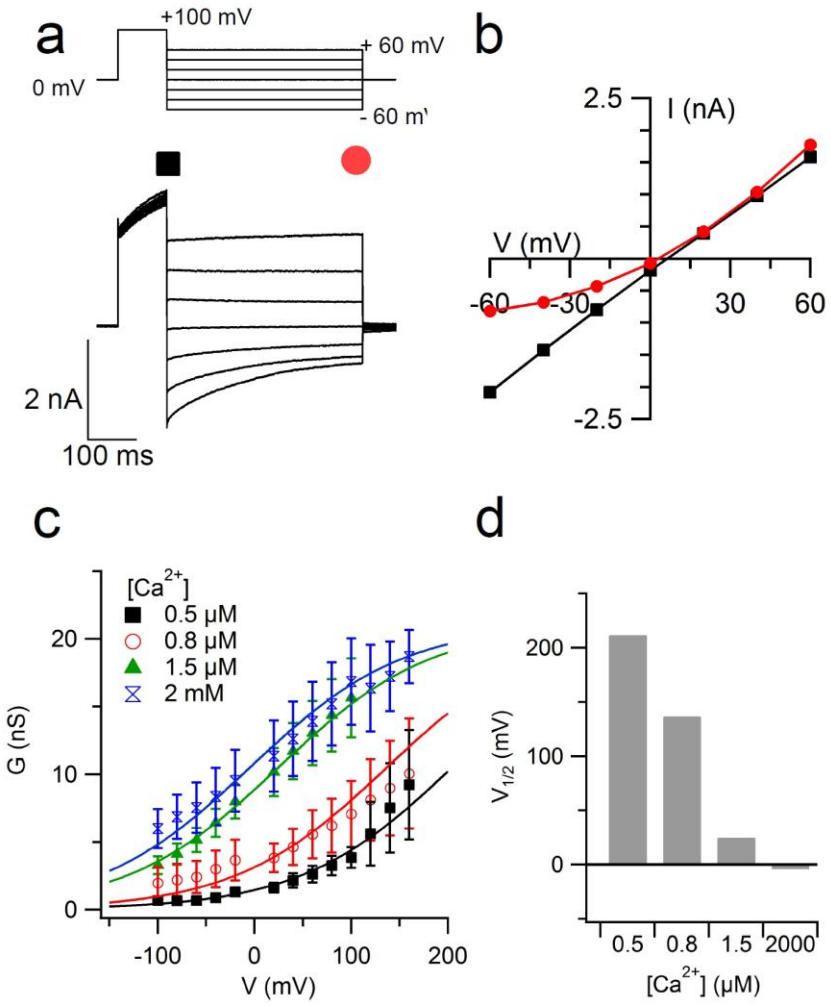

Fig 2: (A) Prepulse of 100ms at +100mV followed by steps from -60 to +60mV in 20 mV increment (top). Currents elicited with 1.5 µM $[Ca^{2+}]_i$ by the indicated prepulse protocol (bottom). **(B)** I-V relations measured from instantaneous tail currents (square) or at the steady state (circles). **(C)** Conductances, calculated from steady-state currents between -100 and +160 mV were plotted versus voltages (n = 3-12). Data were fitted with Boltzmann equation. **(D)** $V_{1/2}$ values were plotted versus $[Ca^{2+}]_i$

Ionic nature of calcium activated current.

To study the ionic nature of the calcium-activated current we changed the ionic composition of extracellular solutions. In a first set of experiments we activated the current with 1.5 µM Ca^{2+} and we reduced the extracellular [Cl^-] to 1 mM. The reversal potential showed a positive shift of 51±7 mV (n=4) demonstrating that the current is mediated by chloride ions (**Fig.3 A-C**). Similar results were obtained with 2 mM of Ca^{2+} in intracellular solution (**Fig.3 C)**. In contrast, the substitution of NaCl with Choline chloride caused a very small change in reversal potential both with 1.5 µM and 2 mM of $[Ca^{2+}]_{i.}$ indicating that the Ca^{2+}-activated current was not mediated by a non-selective cation channel (**Fig.3 D-F**). Finally we replaced extracellular NaCl with NaSCN (**Fig.3 G-I**). This caused a negative shift of the reversal potential of the current indicating that the channels are more permeable to SCN^- than Cl^- as reported for CaCCs (Qu & Hartzell, 2000). Moreover, we observed an increase of conductance in the presence of SCN^-, another typical property of CaCCs (Amédée *et al.*, 1990). Similar results were obtained both with 1.5 µM and 2mM $[Ca^{2+}]_i$ **(Fig.3 I)**

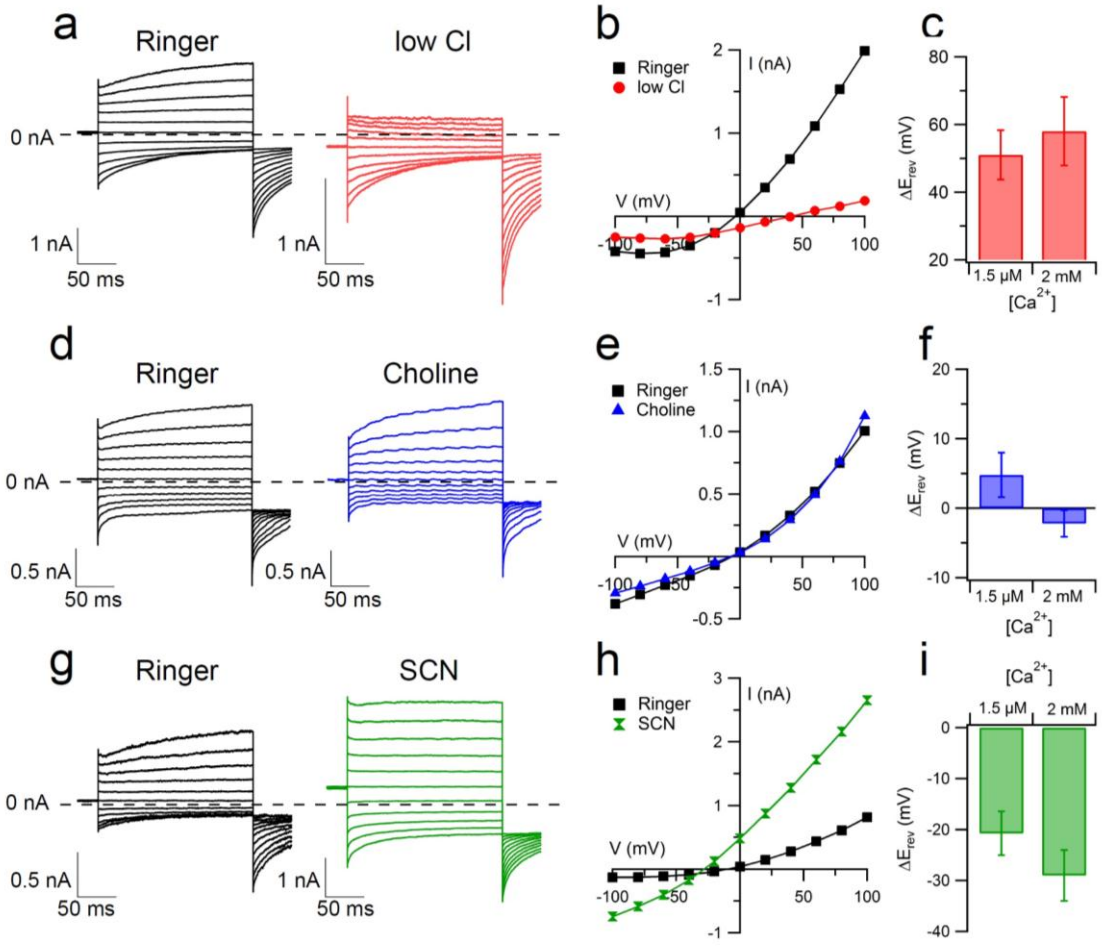

Fig 3: Anion selectivity of Ca^{2+}-activated currents in VSNs. Currents were activated by 1.5μM Ca^{2+} and the same neuron was exposed to solutions containing 140 mM NaCl (black traces) or 1mM NaCl and 139 NaGluconate **(A)**, 140 mM CholineCl **(D)** or 140 mM NaSCN **(G). (B, E, H)** IV plot for the experiments shown in the left columns. Black squares represents control data in NaCl, colored markers refer to low Cl (B), CholineCl (E) and NaSCN (H).**(C, F, I)** Histograms showing the average change in reversal potential respect to the control NaCl bath solution at 1.5μM and 2mM Ca^{2+} in low Cl^- **(C),**CholineCl**(F)** and NaSCN **(I).**

Pharmacology

To assess the pharmacological properties of native calcium activated current we measured the effects of some chloride channel blockers: NFA (300µM) and $CaCC_{inh-A01}$ (10µM) on currents activated by 1.5µM or 2mM $[Ca^{2+}]_i$.

Effect of NFA (300µM)

In previous studies we and others have demonstrated that NFA inhibits calcium-activated chloride currents obtained by flash photolysis of caged Ca^{2+} (Sagheddu *et al.,* 2010; Dibattista *et al.,* 2012). Using the present method of activation, in which defined intracellular Ca^{2+} concentrations were introduced into the neurons via the patch pipette, we investigated the effect of NFA on calcium-activated chloride current activated by different concentration of free $[Ca^{2+}]_i$.

Fig.4 A, C shows that the application of 300µM NFA blocked both the time-dependent outward current and tail component of the current. Inhibition of calcium-activated chloride current by NFA was observed in all the neurons (n= 5-8). The blocking effect of NFA was completely reversible. The IV relations show the decrease in current after the application of NFA **(Fig.4 B, D)**. (**Fig.4 E)** shows the average reduction of the current at -100 and +100mV in the presence of NFA. The blockage of NFA in the presence of both 1.5µM and 2mM $[Ca^{2+}]_i$ was not significantly different.

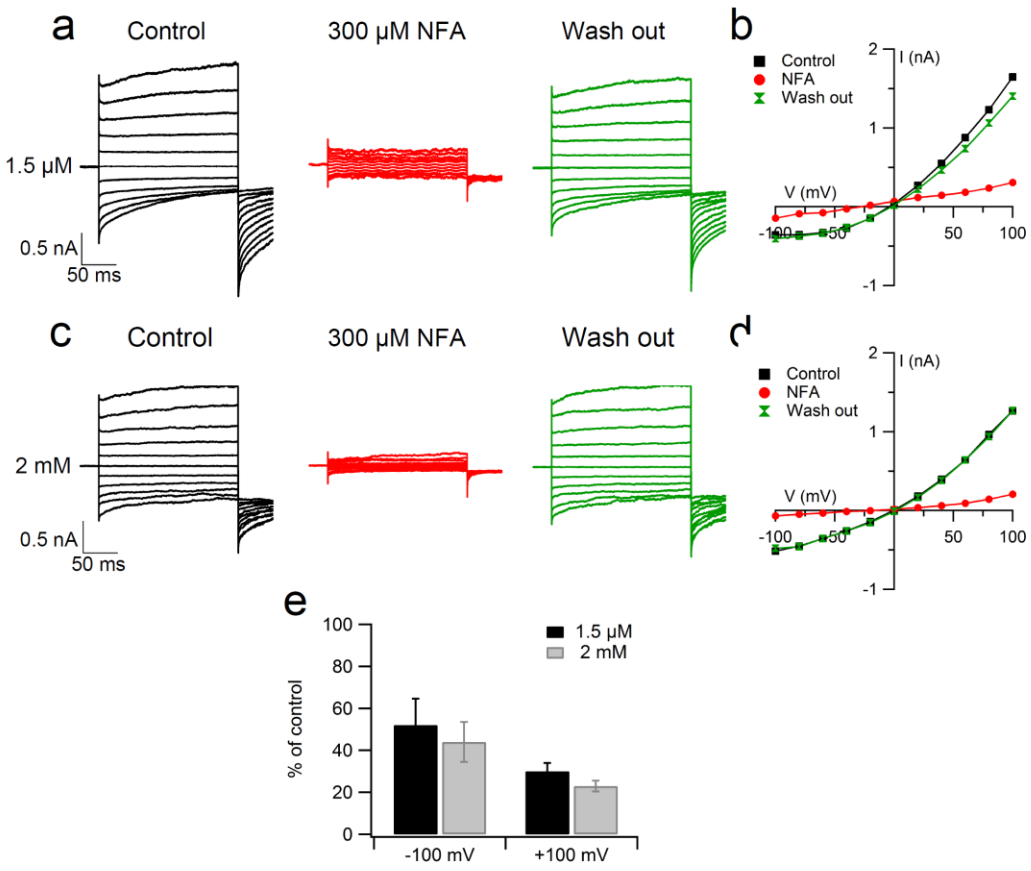

Fig 4: Blockage of the Ca^{2+}-activated current by the chloride channel blocker NFA (300µM). **(A, C)** Whole-cell voltage-clamp recordings obtained with a pipette solution containing 1.5 µM **(A)** or 2mM **(C)** Ca^{2+} in symmetrical Cl^- solutions. Voltage steps of 200 ms duration were given from a holding potential of 0 mV to voltages between −100 and +100 mV in 20 mV steps followed by a step to −100 mV. Current recordings were obtained before blocker application (control), after application of NFA, and 2–5 min after the removal of blockers (washout). **(B, D)** Current voltage relations measured at the end of the voltage steps. **(E)** Average ratios between currents measured in the presence of NFA (300µM) and control measured at −100 mV or at +100 mV at the indicated $[Ca^{2+}]_i$ (n=5-8). Histograms represent mean data ± SEM (n=5-8).

Effect of $CaCC_{inh-A01}$ (10µM)

$CaCC_{inh-A01}$ has recently been indicated as a blocker of CaCC in human airway and intestinal epithelial cell (Namkung *et al.,* 2011). We tested the effect of $CaCC_{inh-A01}$ at 10 µM. **Fig. 5** shows that 10 µM $CaCC_{inh-A01}$ blocked currents in the presence of 1.5µM or 2mM $[Ca^{2+}]_i$ both at negative and positive potentials. The effect of $CaCC_{inh-A01}$ was almost completely reversible **(Fig.5 A, C)**. Current-voltage relations showed a marked decrease in current **(Fig.5 B, D).** On average, the current at +100mV was reduced from 900pA to 343pA at with 1.5µM $[Ca^{2+}]_i$ and from 2493pA to 465pA with 2mM $[Ca^{2+}]_i$ **(Fig.5 E)**.

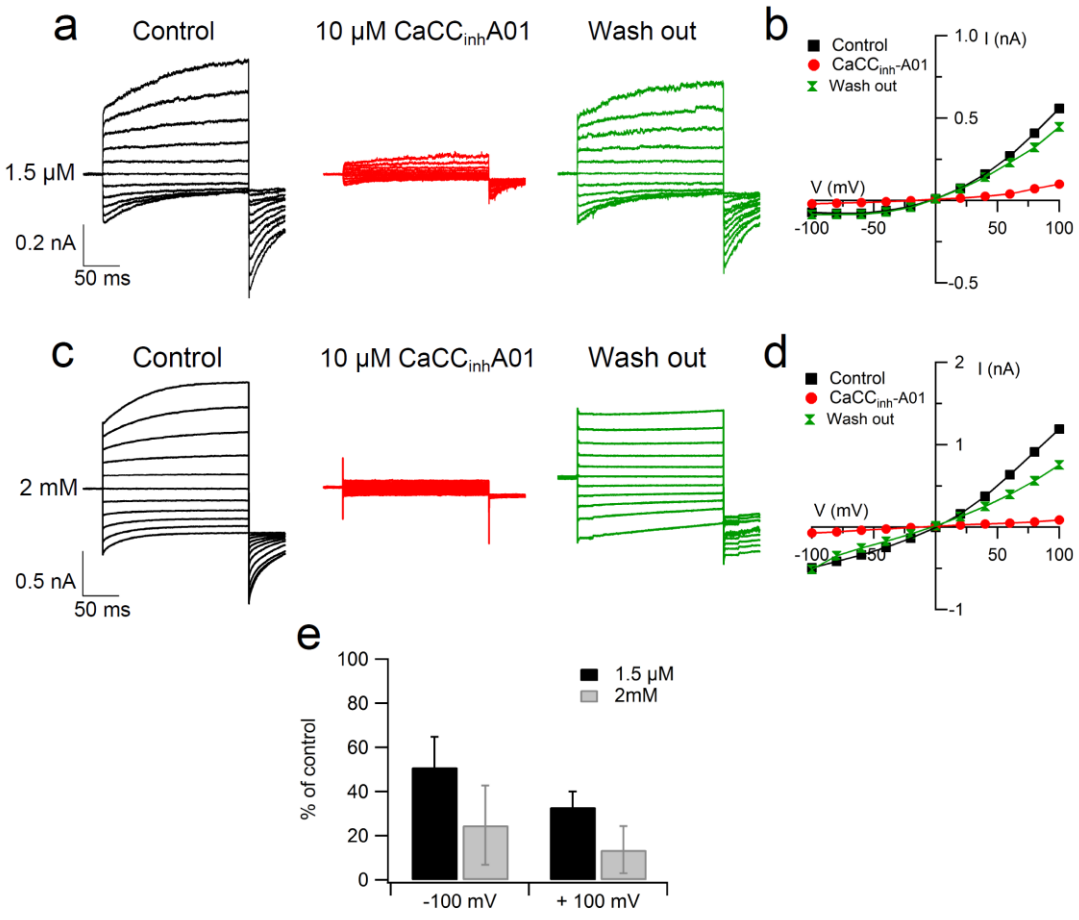

Fig 5: CaCC$_{inh-A01}$ inhibits calcium mediated currents in vomeronasal sensory neurons. **(A & C)** Representative traces of current-mediated by 1.5 µM and 2mM $[Ca^{2+}]_i$. **(B, D)** Current-voltage relations measured at the end of the voltage steps. **(E)** Average ratios between currents in the presence of CaCC$_{inh-A01}$ (10 µM) and control measured at −100 mV or +100 mV at the indicated $[Ca^{2+}]_i$. Average ratios between currents measured at −100 mV or at +100 mV in the presence of CaCC$_{inh-A01}$ at the indicated $[Ca^{2+}]_i$ (n=3-5).

Discussion.

In the present work Ca^{2+}-activated chloride currents are described in isolated VSNs, dialyzed with Ca-HEDTA buffer maintaining a constant intracellular calcium concentration. This experimental approach offers distinct advantages over alternative procedures used to increase the intracellular Ca^{2+} concentrations (Evans & Marty, 1986). A biophysical hallmark of native CaCCs is the phenomenon of "rundown" in excised patches (Pifferi *et al.*, 2009), whereas whole-cell recordings are rather stable so we decided to use the whole-cell patch-clamp configuration. Our results demonstrate the activation of Ca^{2+}-activated chloride current in freshly dissociated mouse VSNs.

First, we have characterized the native CaCC to establish the activation properties. Our whole-cell voltage-clamp studies revealed the presence of a calcium-activated current whose magnitude was steeply dependent on the intracellular free calcium concentration. Most of the freshly isolated cells which we have tested produced outward rectifying currents. We have recorded negligible currents when the concentration of intracellular calcium in the patch pipette was below 10 nM. When $[Ca^{2+}]_i$ was increased, voltage-dependent currents could be activated. The overall characteristic of native Ca^{2+}-activated chloride currents in VSNs are similar to those of heterologous TMEM16A and TMEM16B currents (Yang *et al.*, 2008; Caputo *et al.*, 2008; Schroeder *et al.*, 2008) and, based on our results (Dibattista *et al.*, 2012) TMEM16A and TMEM16B are both expressed in microvilli of mouse VSNs. Indeed, currents measured in heterologous systems expressing TMEM16A or TMEM16B were activated in the micromolar $[Ca^{2+}]_i$ range and exhibited an outward rectification (Caputo *et al.*, 2008; Pifferi *et al.*, 2009). Furthermore the current kinetics properties of CaCCs in VSNs were similar to those of published data on TMEM16A, with current deactivation kinetics in the range of 100ms (Caputo *et al.*, 2008). TMEM16B channels display much faster kinetics of current activation i.e. 4.4ms at +100mV and deactivation 7.1ms at -100mV (Pifferi *et al.*, 2009). Therefore the kinetics characteristic of the native channel closely resemble those of TMEM16A.

In the presence of Ca^{2+}, the dose-response relation for the native CaCC in VSNs was calculated. $K_{1/2}$ value at -100mV was 1.4µM which decreased to 0.6µM at +100mV. The $K_{1/2}$ reported for TMEM16A and TMEM16B has shown variable values. In heterologous expression systems, for TMEM16A in whole-cell recordings $K_{1/2}$ at +100 mV was 332nM (Ferrera *et al.,* 2009) whereas for TMEM16B $K_{1/2}$ at +100 mV was 1.6 µM (Cenedese *et al.,* 2012). These results indicate a lower apparent affinity for Ca^{2+} of TMEM16B compared with TMEM16A. Although there are some differences among studies reported from different laboratories, every study has shown that the apparent affinity for Ca^{2+} is slightly voltage- dependent, with higher apparent Ca^{2+} at positive voltages and the Hill coefficient are consistently higher than one, indicating that more than one Ca^{2+} ion is necessary to activate the channel. The time constant for current activation in VSNs measured at +100mV was 206ms with 0.5µM $[Ca^{2+}]_i$ while the time constant for deactivation at -100mV was 46ms with 0.5µM $[Ca^{2+}]_i$. The time constant for the activation of native CaCC measured in rabbit pulmonary artery, coronary artery and portal vein was 200-300ms while the time constant of deactivation measured in these systems was around 90-100ms (Greenwood *et al.,* 2001). In another study on the native CaCC in pulmonary arterial smooth muscle, the time constant of activation at +70mV was 400ms and time of deactivation was in the range of 100ms (Manoury *et al.,* 2010).

We have shown that TMEM16A and TMEM16B are present in the apical region of mouse VSNs (Dibattista *et al.,* 2012). Some other studies have also shown the presence of CaCCs in VSNs (Yang & Delay, 2010; Kim *et al.,* 2011; Billig *et al.,* 2011). However, the physiological role of these channels in VSNs is still unknown. Chloride equilibrium potential is still not known in the VSNs. Depending on the chloride equilibrium potential, these channels may contribute to the neuron depolarization or hyperpolarization. Perforated patch-clamp recordings showed that the CaCCs act to further amplify the primary inward current indicating that the intracellular chloride concentration is relatively high (Yang & Delay, 2010). In the same paper, the authors have shown that the addition of bumetanide, which is a specific blocker of the sodium potassium-chloride co-transporter (NKCC1),

significantly decreased the urine- induced inward current, which suggests a role for NKCC1 in chloride accumulation within the neuron (Yang & Delay, 2010). The presence of these channels in microvilli of VSNs, where TRPC2 channels are also expressed, gives clue about their contribution to signal transduction. In another study it has been shown that Ca^{2+}-activated chloride current are present also in the TRPC2 knockout mice (Kim *et al.,* 2011). They have suggested that these channels can be activated not only by the Ca^{2+} influx through the TRPC2 channels but also by the Ca^{2+} release from the intracellular stores.

In olfactory sensory neurons the internal chloride concentration is remarkably high. In physiological conditions the opening of CaCCs in olfactory neurons causes an efflux of chloride which contribute to neuron depolarization (Reuter *et al.*,1998; Kaneko *et al.,* 2001; Kaneko *et al.,* 2004). Up to 80% of the total transduction current (Boccaccio and Menini, 2007) is carried by CaCCs, which indicates that these channels may have a role in signal transduction. It is of great interest that the olfactory neurons also expresses TMEM16B at the apical surface, as VSNs, despite the fact that olfactory and vomeronasal neuron show many differences in signal transduction cascades. The expression of TMEM16A and TMEM16B at the site of signal transduction is likely to play a physiological role in sensory transduction.

Conclusion

In the quest of pheromone communication through the vomeronasal neurons many of the ionic mechanisms underlying the signal transduction cascade are still elusive. In the present work we have tried to contribute to the present knowledge of signaling in VSNs by characterizing the CaCC in mice isolated VSNs.

Although the Ca^{2+}-activated chloride currents were described previously in VSNs, however there was no direct evidence of a large Ca^{2+}-activated chloride current in the apical region of mouse VSNs and the co-expression of TMEM16A and TMEM16B in the microvilli of the same sensory neurons. These observations suggest that TMEM16A and TMEM16B are likely to be responsible for the chloride current in VSNs.

In the second part of the thesis we have tried to characterize the properties of CaCCs and found that most of the properties were similar to those of TMEM16A and TMEM16B. However more in depth analysis is still required.

As usual these data raises more questions than the answers they give, our data give the biophysical hints to a bigger picture. It will be interesting to further study the role of CaCCs in TMEM16A and TMEM16B knockout mice.

References

Adams DR, McFarland LZ. "Septal olfactory organ in Peromyscus." *Comp Biochem Physiol A* (1971); 40(4): 971–74.

Agnel M, Vermat T, Culouscou JM. "Identification of three novel members of the calcium-dependent chloride channel (CaCC) family predominantly expressed in the digestive tract and trachea." *FEBS Lett.* (1999); 455(3): 295-301.

Amédée T, Large WA, Wang Q. "Characteristics of chloride currents activated by noradrenaline in rabbit ear artery cells." *J Physiol* (1990); 428: 501-16.

Bader CR, Bertrand D, Schlichter R. "Calcium-activated chloride current in cultured sensory and parasympathetic quail neurones." *J Physiol.* (1987); 394: 125-48.

Bader CR, Bertrand D, Schwartz EA. "Voltage-activated and calcium-activated currents studied in solitary rod inner segments from the salamander retina." *J Physio* (1982); 331: 253-84.

Barish ME. "A transient calcium-dependent chloride current in the immature Xenopus oocyte." *J Physiol.* (1983); 342: 309-25.

Bellringer JF, Pratt HP & Keverne EB. " Involvement of the vomeronasal organ and prolactin in pheromonal induction of delayed implantation in mice." *J Reprod Fertil* (1980); 59(1): 223-228.

Bera TK, Das S, Maeda H, Beers R, Wolfgang CD, Kumar V, Hahn Y, Lee B, Pastan I. "NGEP, a gene encoding a membrane protein detected only in prostate cancer and normal prostate." *Proc Natl Acad Sci U S A.* (2004); 101(9): 3059-64.

Berecki G, Varga Z, Van Iren F, Van Duijn B. "Anion channels in chara corallina tonoplast membrane: calcium dependence and rectification." *J Membr Biol.* (1999); 172(2): 159-68.

Berghard A, Buck LB. "Sensory transduction in vomeronasal neurons: evidence for G alpha o, G alpha i2, and adenylyl cyclase II as major components of a pheromone signaling cascade." *J Nerosci* (1996); 16(3): 909–918.

Billig GM., Pál B, Fidzinski P, and Jentsch TJ. "Ca2+-activated Cl currents are indespensable for olfaction." *Nat. Neurosci* (2011); 14(6): 763–769.

Boccaccio A & Menini A. "Temporal development of cyclic neuclotide-gated and Ca2+ activated Cl- current in isolated mouse olfactory sensory neurons" *J Neurophysiol* (2007); 98(1): 153-60

Boschat C, Pélofi C, Randin O, Roppolo D, Lüscher C, Broillet MC, Rodriguez I. "Pheromone detection mediated by a V1r vomeronasal receptor." *Nat Neurosci.* (2002); 5(12): 1261-2.

Brechbühl J, Klaey M & Broillet MC. "Grueneberg ganglion cells mediate alarm pheromone detection in mice." *Science* (2008); 321 (5892): 1092-1095.

Brechbühl J, Moine F, Klaey M, Nenniger-Tosato M, Hurni N, Sporkert F, Giroud C, Broillet MC. "Mouse alarm pheromone shares structural similarity with predator scents." *Proc Natl Acad Sci* (2013); 110(12): 4762-4767.

Breipohl W, Naguro T., Miragall F. "Morphology of the Masera organ in NMRI mice (combined morphometric, freeze-fracture, light- and scanning electron microscopic investigations." *Verh Anat Ges* (1983); 77: 741–43.

Breipohl W, Naguro T., Walker D.G. The postnatal development of Maresa's organ in the rat. *Chem Senses*. 1989; 14: 649–62.

Buck L & Axel R. "A novel multigene family may encode odorant receptors: a molecular basis for odor recognition." *Cell* (1991); 65(1): 175–187.

Butenandt A, Beckmann R., Stamm D., Hecker E,. "Über den Sexual-Lockstoff des Seidenspinners Bombyx mori." *Zeitschrift für Naturforschung Teil B* (1959): 283–284.

Caputo A, Caci E., Ferrera L., Pedemonte N., Barsanti C. "TMEM16A, a membrane protein associated with calcium-dependent chloride channel activity." *Science* (2008); 322(5901): 590–594.

Cenedese V, Betto G, Celsi F, Cherian OL, Pifferi S, Menini A. "The voltage dependence of the TMEM16B/anoctamin2 calcium-activated chloride channel is modified by

mutations in the first putative intracellular loop." *J Gen Physiol.* (2012); 139(4): 285-94.

Chamero P, Marton T.F., Logan D.W., Flanagan K., Cruz J.R., Saghatelian A., Cravatt B.F., Stowers L. "Identification of protein pheromones that promote aggressive behaviour. ." *Nature.* (2007); 450(7171): 899–902.

Ciges M, Labella T, Gayoso M & Sanchez G. "Ultrastructure of the organ of Jacobson and comparative study with olfactory mucosa." *Acta Otolaryngol* (1977); 83(1-2): 47-58.

Cinelli AR, Wang D, Chen P, Liu W, Halpern M. "Calcium transients in the garter snake vomeronasal organ." *J Neurophysiol* (2002); 87(3): 1449-72.

Clapham DE & Neer EJ . "G protein beta gamma subunits." *Annu Rev Pharmacol Toxicol* (1997); 37: 167-203.

Cross NL & Elinson RP. "A fast block to polyspermy in frogs mediated by changes in the membrane potential." *Dev Biol.* (1980); 75(1): 187-98.

Cross NL. "Initiation of the activation potential by an increase in intracellular calcium in eggs of the frog, Rana pipiens." *Dev Biol.* (1981); 85(2): 380-4.

Cunningham SA, Awayda MS, Bubien JK, Ismailov II, Arrate MP, Berdiev BK, Benos DJ, Fuller CM. "Cloning of an epithelial chloride channel from bovine trachea." *J Biol Chem.* (1995); 270(52): 31016-26.

Currie KP, Wootton JF, Scott RH. "Activation of Ca(2+)-dependent Cl^- currents in cultured rat sensory neurones by flash photolysis of DM-nitrophen." *J Physiol.* (1995); 482(2): 291-307.

Das S, Hahn Y, Nagata S, Willingham MC, Bera TK, Lee B, Pastan I. "NGEP, a prostate-specific plasma membrane protein that promotes the association of LNCaP cells." *Cancer Res.* (2007); 67(4): 1594-601.

De Castro F, Geijo-Barrientos E, Gallego R. "Calcium-activated chloride current in normal mouse sympathetic ganglion cells." *J Physiol.* (1997); 498(2): 397-408.

Del Punta K, Leinders-Zufall T, Rodriguez I, Jukam D, Wysocki CJ, Ogawa S, Zufall F, Mombaerts P. "Deficient pheromone responses in mice lacking a cluster of vomeronasal receptor genes." *Nature*. (2002); 419(6902): 70-4.

Dennis JC, Allgier JG, Desouza LS, Eward WC, Morrison EE. "Immunohistochemistry of the canine vomeronasal organ." *J Anat* (2003); 203(3): 329-38.

Dibattista M, Mazzatenta A, Grassi F, Tirindelli R & Menini A. "Hyperpolarization-activated cyclic nucleotide-gated channels in mouse vomeronasal sensory neurons." *J Neurophysiol* (2008); 100(2): 576-586.

Dibattista M, Amjad A, Maurya DK, Sagheddu C, Montani G, Tirindelli R, Menini A. "Calcium-activated chloride channels in the apical region of mouse vomeronasal sensory neurons." *J Gen Physiol* (2012); 140(1): 3-15.

Døving KB & Trotier D. "Structure and function of the vomeronasal organ." *J. Exp. Biol.* (1998); 201: 2913–25.

Dulac C & Axel R. "A novel family of genes encoding putative pheromone receptors in mammals." *Cell* (1995); 83(2): 195–206.

Duran C, Qu Z, Osunkoya AO, Cui Y, Hartzell HC. "ANOs 3-7 in the anoctamin/Tmem16 Cl- channel family are intracellular protein." *Am J Physiol Cell Physiol* (2012); 302(3): 482-93.

Eisthen HL. "The Goldfish Knows: Olfactory Receptor Cell Morphology Predicts Receptor Gene Expression." *J Comp Neurol*. (2004); 477(4): 341–346.

Elble RC, Widom J, Gruber AD, Abdel-Ghany M, Levine R, Goodwin A, Cheng HC, Pauli BU. "Cloning and characterization of lung-endothelial cell adhesion molecule-1 suggest it is an endothelial chloride channel." *J Biol Chem* (1997); 272(44): 27853-61.

Elsaesser R, Montani G, Tirindelli R, Paysan J. "Phosphatidyl-inositide signalling proteins in a novel class of sensory cells in the mammalian olfactory epithelium." *Eur J Neurosci* (2005); 21(10): 2692-700.

Estes RD. "The role of the vomeronasal organ in mammalian reproduction." *Mammalia* (1972); 36(3): 315-341.

Evans MG, Marty A. "Calcium-dependent chloride currents in isolated cells from rat lacrimal glands." *J Physiol.* (1986); 378: 437-60.

Fallah G, Römer T, Detro-Dassen S, Braam U, Markwardt F, Schmalzing G. "TMEM16A(a)/anoctamin-1 shares a homodimeric architecture with CLC chloride channels." *Mol Cell Proteomics* (2011); 10(2) : M110.001697.

Ferrera L, Caputo A, Ubby I, Bussani E, Zegarra-Moran O, Ravazzolo R, Pagani F, Galietta LJ. "Regulation of TMEM16A chloride channel properties by alternative splicing." *J Biol Chem* (2009); 284(48): 3360-8.

Fieni F, Ghiaroni V, Tirindelli R, Pietra P & Bigiani A. "Apical and basal neurones isolated from the mouse vomeronasal organ differ for voltage-dependent currents." *J Physiol* (2003); 552(Pt 2): 425-436.

Fleischer J, Hass N, Schwarzenbacher K, Besser S, Breer H. "A novel population of neuronal cells expressing the olfactory marker protein (OMP) in the anterior/dorsal region of the nasal cavity." *Histochem Cell Biol.* (2006); 125(4): 337-49.

Frings S, Reuter D, Kleene SJ. "Neuronal Ca2+ -activated Cl- channels--homing in on an elusive channel species." *Prog Neurobiol* (2000); 60(3): 247-89.

Fromm J, Lautner S. "Electrical signals and their physiological significance in plants." *Plant Cell Environ* (2007); 30(3): 249-57.

Fuss SH, Omura M, Mombaerts P. "The Grueneberg ganglion of the mouse projects axons to glomeruli in the olfactory bulb." *Eur J Neurosc* (2005); 22(10): 2649-2654.

Gandhi R, Elble RC, Gruber AD, Schreur KD, Ji HL, Fuller CM, Pauli BU. "Molecular and functional characterization of a calcium-sensitive chloride channel from mouse lung." *J Biol Chem* (1998); 273(48): 32096-101.

Giacobini P, Benedetto A, Tirindelli R, Fasolo A. "Proliferation and migration of receptor neurons in the vomeronasal organ of the adult mouse." *Brain Res* (2000); 123(1): 33–40.

Greenwood IA, Ledoux J, Leblanc N. "Differential regulation of Ca(2+)-activated Cl(-) currents in rabbit arterial and portal vein smooth muscle cells by Ca(2+)-calmodulin-dependent kinase." *J Physiol.* (2001); 532(Pt-2): 395-408.

Grosmaitre X, Santarelli L.C., Tan J., Luo M., Ma M. "Dual functions of mammalian olfactory sensory neurons as odor detectors and mechanical sensors." *Nat Neurosc* (2007); 10(3): 348–54.

Grubb S, Poulsen KA, Juul CA, Kyed T, Klausen TK, Larsen EH, Hoffmann EK. "TMEM16F (Anoctamin 6), an anion channel of delayed Ca(2+) activation." *J Gen Physiol.* (2013); 141(5): 585-600.

Gruber AD, Elble RC, Ji HL, Schreur KD, Fuller CM, Pauli BU. "Genomic cloning, molecular characterization, and functional analysis of human CLCA1, the first human member of the family of Ca2+-activated Cl- channel proteins." *Genomics.* (1998); 54(2): 200-14.

Gruber AD, Gandhi R, Pauli BU. "The murine calcium-sensitive chloride channel (mCaCC) is widely expressed in secretory epithelia and in other select tissues." *Histochem Cell Biol* (1998); 110(1): 43-9.

Gruber AD, Pauli BU. "Molecular cloning and biochemical characterization of a truncated secreted member of the human family of Ca2+-activated Cl− channels." *Biochim. Biophys. Acta* (1998); 1444(3): 418-23.

Grüneberg, Hans. "A ganglion probably belonging to the N. terminalis system in the nasal mucosa of the mouse." *Zeitschrift für Anatomie und Entwicklungsgeschichte* (1973); 140(1): 39-52.

Halpern M, Martínez-Marcos A. "Structure and function of the vomeronasal system: An update." *Prog. Neurobiol.* (2003); 70(3): 245–318.

Hartzell C, Putzier I, Arreola J. "Calcium-activated chloride channels." *Annu Rev Physiol* (2005); 67: 719-58.

Hartzell HC, Qu Z, Yu K, Xiao Q, Chien LT. "Molecular physiology of bestrophins: multifunctional membrane proteins linked to best disease and other retinopathies." *Physiol Rev*. (2008); 88(2): 639-72.

Herness MS, Sun XD. "Characterization of chloride currents and their noradrenergic modulation in rat taste receptor cells." *J Neurophysiol.* (1999); 82(1): 260-71.

Herrada G & Dulac C. " A novel family of putative pheromone receptors in mammals with a topographically organized and sexually dimorphic distribution." *Cell* (1997); 90(4): 763–773.

Holy TE, Dulac C & Meister M. "Responses of vomeronasal neurons to natural stimuli." *Science* (2000); 289(5484): 569-1572.

Huang F, Wong X, Jan LY. "International Union of Basic and Clinical Pharmacology. LXXXV: calcium-activated chloride channels." *Pharmacol Rev.* (2012); 16(1): 1-15.

Hudson R, Distel H. "Pheromonal release of suckling in rabbits does not depend on the vomeronasal organ." *Physiol Behav* 37 (1986); 37(1): 123-128.

Hurst J, Beynon R. "Scent wars: The chemobiology of competitive signalling in mice." *Bioessays* (2004); 26(12): 1288–98.

Hussy N. "Developmental change in calcium-activated chloride current during the differentiation of Xenopus spinal neurons in culture." *Dev Biol.* (1991); 147(1): 225-38.

Hussy N. "Calcium-activated chloride channels in cultured embryonic Xenopus spinal neurons." *J Neurophysiol* (1992); 68(1): 2042-50.

Inamura K, Kashiwayanagi M, Kurihara K. "Inositol-1,4,5-trisphosphate induces responses in receptor neurons in rat vomeronasal sensory slices." *Chem Sense* (1997); 22(1): 93-103.

Inamura K, Kashiwayanagi M. "Inward current responses to urinary substances in rat vomeronasal sensory neurons." *Eur J Neurosci.* (2000); 12(10): 3529-36.

Ishii T, Hirota J & Mombaerts P. "Combinational coexpression of neural and immune multigene families in mouse vomeronasal sensory systems." *Curr. Biol* (2003); 13(5): 394–400.

Jentsch TJ, Stein V, Weinreich F, Zdebik AA. "Molecular structure and physiological function of chloride channels." *Physiol Rev.* (2002); 82(2): 503-68.

Johnston RE. "Vomeronasal and/or olfactory mediation of ultrasonic calling and scent marking by female golden hamsters." *Physiol Behav* (1992); 51(2): 437-448.

Kaneko H, Nakamura, Lindemann B. "Noninvasive measurement of chloride concentration in rat olfactory receptor cells with use of a fluorescent dye. *Am J Physiol* (2001); 280(6): C1387-93

Kaneko H, Putzier I, Frings S, Kaupp UB, Gensch T. "Chloride accumulation in mammalian olfactory sensory neurons. *J Neurosci* (2004); 24(36): 7931-8

Katz S, Merzel J. "Distribution of epithelia and glands of the nasal septum mucosa in the rat." *Acta Anat (Basel)* (1977); 99(1): 58–66.

Kelliher KR, Spehr M, Li XH, Zufall F, Leinders-Zufall T. "Pheromonal recognition memory induced by TRPC2-independent vomeronasal sensing." *Eur J Neurosci* (2006); 23(1): 3385–3390.

Kelly DR. "When is a butterfly like an elephant? ." *Chem. Biol* (1996); 3(8): 595-602.

Kim S, Ma L, Yu CR. "Requirement of calcium-activated chloride channels in the activation of mouse vomeronasal neurons." *Nat Commun* (2011); 2(365).

Kleene SJ & Gesteland RC. "Calcium-activated chloride conductance in frog olfactory cilia." *J Neurosci.* (1991); 11(11): 3624-9.

Kleene SJ. "The electrochemical basis of odor transduction in vertebrate olfactory cilia." *Chem Senses* (2008); 33(9): 839-59.

Koos DS, Fraser SE. "The Grueneberg ganglion projects to the olfactory bulb." *Neuroreport* (2005); 16(17): 1929-1932.

Koumi S, Sato R, Aramaki T. "Characterization of the calcium-activated chloride channel in isolated guinea-pig hepatocytes." *J Gen Physiol.* (1994); 104(2): 357-73.

Krieger J, Schmitt A, Lobel D, Gudermann T, Schultz G, Breer H, Boekhoff I. "Selective activation of G protein subtypes in the vomeronasal organ upon stimulation with urine-derived compounds." *J Biol Chem* (1999); 274(8): 4655–4662.

Kubie JL & Halpern M. "The chemical senses involved in garter snake prey trailing." *Neurosci. Abs* (1976); 93(4): 148.

Kurahashi T, Kaneko A. "High density cAMP-gated channels at the ciliary membrane in the olfactory receptor cell." *Neuroreport* (1991);2(1): 5-8.

Large WA, Wang Q. "Characteristics and physiological role of the Ca(2+)-activated Cl- conductance in smooth muscle." *Am J Physiol.* (1996); 271 (2 pt 1): 435-54.

Leinders-Zufall T, Brennan P, Widmayer P, PC S, Maul-Pavicic A, Jäger M, Li XH, Breer H, Zufall F, Boehm T. "MHC class I peptides as chemosensory signals in the vomeronasal organ." *Science* (2004); 306(5698): 1033-37.

Leinders-Zufall T., Lane A.P., Puche A.C., Ma W., Novotny M.V., Shipley M.T., Zufall F. " Ultrasensitive pheromone detection by mammalian vomeronasal neurons." *Nature* (2000); 405(6788): 792-96.

Leypold BG, Yu CR, Leinders-Zufall T, Kim MM, Zufall F, Axel R. "Altered sexual and social behaviors in trp2 mutant mice." *Proc Natl Acad Sci* (2002); 99(9): 6376–6381.

Librles SD, Horowitz LF, Kuang D, Contos JJ, Wilson KL, Siltberg-Liberles J, Liberles DA, Buck LB. "Formyl peptide receptors are candidate chemosensory receptors in the vomeronasal organ" *Proc Natl Acad Sci U S A* (2009); 106(24): 9842-7.

Liman ER. "Regulation by voltage and adenine nucleotides of a Ca2+-activated cation channel from hamster vomeronasal sensory neurons." *J Physiol* (2003); 548(Pt 3): 777–787.

Liman ER, Corey DP, Dulac C. "TRP2: a candidate transduction channel for mammalian pheromone sensory signaling." *Proc Natl Acad Sci* (1999); 96(10): 5791–5796.

Liman ER, Corey DP. "Electrophysiological characterization of chemosensory neurons from the mouse vomeronasal organ." *J Neurosci* (1996); 16(15): 4625–4637.

Lin DY, Zhang S.-Z., Block E., Katz L.C. " Encoding social signals in the mouse main olfactory bulb." *Nature* (2005); 434(7032): 470–77.

Loebel D, Scaloni A., Paolini S., Fini C., Ferrara L., Breer H., Pelosi P. " Cloning, post-translational modifications, heterologous expression and ligand-binding of boar salivary lipocalin." *Biochem. J.* (2000); 350(Pt 2): 369–79.

Lucas P, Ukhanov K, Leinders-Zufall T, Zufall F. "A diacylglycerol-gated cation channel in vomeronasal neuron dendrites is impaired in TRPC2 mutant mice: mechanism of pheromone transduction." *Neuron* (2003); 40(3): 551-61.

Karlson P & Luscher M. "Pheromones': a new term for a class of biologically active substances." *Nature* (1959); 183(4653): 55-56.

Mägert HJ, Cieslak A., Alkan O., Lüscher B., Kauffels W., Forssmann W.-G. "The golden hamster aphrodisin gene." *J. Biol. Chem.* (1999); 274: 444–50.

Manoury B, Tamuleviciute A, Tammaro P. "TMEM16A/anoctamin 1 protein mediates calcium-activated chloride currents in pulmonary arterial smooth muscle cells." *J Physiol*. (2010); 588(Pt 13): 2305-14.

Maricq AV, Korenbrot JI. "Calcium and calcium-dependent chloride currents generate action potentials in solitary cone photoreceptors." *Neuron* (1988); 1(16): 503-15.

Marshall DA & Maruniak J.A. "Masera's organ responds to odorants." *Brain Res* (1986); 366(1-2): 329–32.

Matsunami H, Buck LB. "A multigene family encoding a diverse array of putative pheromone receptors in mammals." *Cell* (1997); 90(4): 775–784.

Mayer ML. "A calcium-activated chloride current generates the after-depolarization of rat sensory neurones in culture." *J Physiol*. (1985); 364: 217-39.

McBride DW Jr & Roper SD. "Ca(2+)-dependent chloride conductance in Necturus taste cells." *J Membr Biol.* (1991); 124(1): 85-93.

McCotter RE. "The connection of the vomeronasal nerves with the accessory olfactory bulb in the oppossum and other mammals." *Anat. Rec* (1912); 6(8): 299-318.

Menco BP, Carr VM, Ezeh PI, Liman ER, Yankova MP. "Ultrastructural localization of G-proteins and the channel protein TRP2 to microvilli of rat vomeronasal receptor cells." *J Comp Neurol* (2001); 438(4): 468–489.

Meredith, M. & Burghardt, G. M. "Electrophysiological studies of the tongue and accessory olfactory bulb in garter snakes." *Phyeiol. & Behav*. (1978); 21(6): 1001-8.

Migeotte I, Communi D & Parmentier M. "Formyl peptide receptors: a promiscuous subfamily of G protein-coupled receptors controlling immune responses. ." *Cytokine Growth Factor Rev* (2006); 17(6): 501-519.

Miledi R & Parker I. "Chloride current induced by injection of calcium into Xenopus oocytes." *J Physiol.* (1984); 357: 173–183.

Minke B & Cook B. "TRP channel proteins and sigal transduction." *Physiol Rev* (2002); 82(2): 429-72.

Mombaerts P, Wang F., Dulac C., Chao S.K., Nemes A., Mendelsohn M., Edmondson J., Axel R. "Visualizing an olfactory sensory map." *Cell* (1996); 87(4): 675–86.

Namkung W, Phuan PW, Verkman AS. "TMEM16A inhibitors reveal TMEM16A as a minor component of calcium-activated chloride channel conductance in airway and intestinal epithelial cells." *J Biol Chem* (2011); 286(3): 2365-74.

Nilius B, Vennekens R. "From cardiac cation channels to the molecular dissection of the transient receptor potential channel TRPM4." *Pflügers Arch* (2006); 453(3): 313–32.

Nodari F, Hsu F.F., Fu X., Holekamp T.F., Kao L.F., Turk J., Holy T.E. "Sulfated steroids as natural ligands of mouse pheromone-sensing neurons." *J. Neurosci.* (2008); 28(25): 6407–18.

Norlin EM, Gussing F & Berghard A. "Vomeronasal phenotype and behavioral alterations in G alpha i2 mutant mice." *Curr Biol* (2003); 13(14): 1214-1219.

Novotny MV. "Pheromones, binding proteins and receptor responses in rodents." *Biochem. Soc. Trans* (2003); 31(Pt1): 117–22.

Pantages E, Dulac C. "A novel family of candidate pheromone receptors in mammals." *Neuron* (2000); 28(3): 835-45.

Papassotiriou J, Eggermont J, Droogmans, G, Nilius B. " Ca2+-activated Cl−channels in Ehrlich ascites tumor cells are distinct from mCLCA1, 2 and 3." *Pfluger Arch* (2001); 442(2): 273–79.

Pauli BU, Abdel-Ghany M, Cheng HC, Gruber AD, Archibald HA, Elble RC. "Molecular characteristics and functional diversity of CLCA family members." *Clin. Exp. Pharmacol. Physio* (2000); 27(11): 901–5.

Petrukhin K, Koisti MJ, Bakall B, Li W, Xie G, Marknell T, Sandgren O, Forsman K, Holmgren G, Andreasson S, Vujic M, Bergen AA, McGarty-Dugan V, Figueroa D, Austin CP, Metzker ML, Caskey CT, Wadelius C. "Identification of the gene responsible for Best macular dystrophy." *Nat Genet* (1998); 19(3): 241-7.

Pifferi S, Dibattista M, Sagheddu C, Boccaccio A, Al Qteishat A, Ghirardi F, Tirindelli R, Menini A. "Calcium-activated chloride currents in olfactory sensory neurons from mice lacking bestrophin-2." *J Physiol.* (2009b); 587(17): 4265-79.

Pifferi S., Dibattista M, Menini A. "TMEM16B induces chloride currents activated by calcium in mammalian cells." *Pflugers Arch* (2009); 458(6): 1023-38.

Qu Z, Fischmeister R, Hartzell C. "Mouse bestrophin-2 is a bona fide Cl(-) channel: identification of a residue important in anion binding and conduction." *J Gen Physiol.* (2004); 123(4): 327-40.

Qu Z, Hartzell HC. "Anion permeation in Ca(2+)-activated Cl(-) channels." *J Gen Physiol* (2000); 116(6): 825-44.

Ressler KJ, Sullivan S.L., Buck L.B. "A zonal organization of odorant receptor gene expression in the olfactory epithelium." *Cell* (1993); 73(3): 597–609.

Reuter D, Zierold K, Schröder WH, Frings S. "A depolarizing chloride curret contributes to the chemoelectrical transduction in olfactory sensory neurons in situ." *J Neurosci* (1998); 18(17): 6623-30.

Ricardo De La Fuente, Wan Namkung, Aaron Mills and A. S. Verkman. "Small-Molecule Screen Identifies Inhibitors of a Human Intestinal Calcium-Activated Chloride Channel." *Molecular Pharmacology* (2009); 73(3): 758-768.

Rodolfo-Masera T. "Su 1'esistenza di un particolare organo olfattivo nel setto nasale della cavia e di altri roditori." *Arch Ital Anat Embryol* (1943); 48: 157–212.

Romanenko VG, Catalán MA, Brown DA, Putzier I, Hartzell HC, Marmorstein AD, Gonzalez-Begne M, Rock JR, Harfe BD, Melvin JE. "Tmem16A encodes the Ca2+-activated Cl- channel in mouse submandibular salivary gland acinar cells." *J Biol Chem.* (2010); 285(17): 12990-3001.

Roppolo D, Ribaud V, Jungo VP, Luscher C & Rodriguez I. "Projection of the Gruneberg ganglion to the mouse olfactory bulb." *Eur J Neurosci* (2006); 23(11): 2887-2894.

Ryba NJ, Tirindelli R. "A new multigene family of putative pheromone receptors." *Neuron* (1997); 19(2): 371–379.

Sagheddu C, Boccaccio A, Dibattista M, Montani G, Tirindelli R, Menini A. "Calcium concentration jumps reveal dynamic ion selectivity of calcium-activated chloride currents in mouse olfactory sensory neurons and TMEM16b-transfected HEK 293T cells." *he Journal of Physiology* (2010); 588(Pt21): 4189-4204.

Sanders KM, Koh SD, Ward SM. "Interstitial cells of Cajal as pacemakers in the gastrointestinal tract." *Annu Rev Physiol.* (2006); 68: 307-43.

Schild D, Restrepo D. "Transduction mechanisms in vertebrate olfactory receptor cells." *Physiol Rev* (1998); 78(2): 429-466.

Schlichter LC, Elinson RP. "Electrical responses of immature and mature Rana pipiens oocytes to sperm and other activating stimuli." *Dev Biol.* (1981); 83(1): 33-41.

Schroeder BC, Cheng T, Jan YN, Jan LY. "Expression cloning of TMEM16A as a calcium-activated chloride channel subunit." *Cell* (2008); 134(6): 1019–1029.

Scott RH, McGuirk SM, Dolphin AC. "Modulation of divalent cation-activated chloride ion currents." *Br J Pharmacol.* (1988); 94(3): 653-62.

Sheridan JT, Worthington EN, Yu K, Gabriel SE, Hartzell HC, Tarran R. "Characterization of the oligomeric structure of the Ca(2+)-activated Cl- channel Ano1/TMEM16A." *J Biol Chem.* (2011); 286(2): 1381-8.

Shi P, Zhang J. "Comparative genomic analysis identifies an evolutionary shift of vomeronasal receptor gene repertoires in the vertebrate transition from water to land." *Genome Res* (2007); 17(2): 166–74.

Shimazaki R, Boccaccio A, Mazzatenta A, Pinato G, Migliore M & Menini A. "Electrophysiological properties and modeling of murine vomeronasal sensory neurons in acute slice preparations." *Chemical Senses* (2006); 31(5): 425-435.

Spehr J, Hagendorf S, Weiss J, Spehr M, Leinders-Zufall T & Zufall F. "Ca2+-calmodulin feedback mediates sensory adaptation and inhibits pheromone-sensitive ion channels in the vomeronasal organ." *Journal of Neuroscience* (2009); 29(7): 2125-2135.

Spehr J, Hagendorf S, Weiss J, Spehr M, Leinders-Zufall T, Zufall F. "Ca2+-calmodulin feedback mediates sensory adaptation and inhibits pheromone-sensitive ion channels in the vomeronasal organ." *J Neurosci* (2009); 29(7): 2125–2135.

Spehr M, Hatt H, Wetzel CH. "Arachidonic acid plays a role in rat vomeronasal signal transduction. ." *J Neurosci* (2002) 22(19): 8429–8437.

Stapleton SR, Scott RH, Bell BA. "Effects of metabolic blockers on Ca(2+)-dependent currents in cultured sensory neurones from neonatal rats." *Br J Pharmacol.* (1994); 111(1): 57-64.

Stephan AB, Shum EY., Hirsh S., Cygnar KD. Reisert J. Zhao H. "ANO2 is the cilial calcium-activated chloride channel that may mediate olfactory amplification." *Proc. Natl. Acad. Sci.* (2009) 106(28): 11776–11781.

Stern K, McClintock MK. "Regulation of ovulation by human pheromones." *Nature* (1998); 392(6672): 177-9.

Stowers L, Holy TE, Meister M, Dulac C, Koentges G. "Loss of sex discrimination and male-male aggression in mice deficient for TRP2. ." *Science* (2002); 295(5559): 1493–1500.

Sun H, Tsunenari T, Yau KW, Nathans J. "The vitelliform macular dystrophy protein defines a new family of chloride channels." *Proc Natl Acad Sci U S A* (2002); 99(6): 4008-13.

Suzuki J, Umeda M, Sims PJ, Nagata S. "Calcium-dependent phospholipid scrambling by TMEM16F." *Nature* (2010); 468(7325): 834–838.

Tachibana T, Fujiwara N, Nawa T. "The ultrastructure of the ganglionated nerve plexus in the nasal vestibular mucosa of the musk shrew (Suncus murinus, insectivora)." *Arch Histol Cytol* (1990); 53(2): 147-156.

Tanaka M, Treloar H, Kalb RG, Greer CA & Strittmatter SM . "G(o) protein dependent survival of primary accessory olfactory neurons." *Proc Natl Acad Sci* (1999); 96(24): 14106-14111.

Taylor R, Roper S. "Ca(2+)-dependent Cl- conductance in taste cells from Necturus." *J Neurophysiol.* (1994); 72(1): 475-8.

Tirindelli R, Dibattista M, Pifferi S, Menini A. "From pheromones to behavior." *Physiol Rev.* (2009); 89(3): 921-56.

Tsunenari T, Nathans J, Yau KW. "Ca2+-activated Cl- current from human bestrophin-4 in excised membrane patches." *J Gen Physiol.* (2006);127(6) :749-54.

Tsunenari T, Sun H, Williams J, Cahill H, Smallwood P, Yau KW, Nathans J. "Structure-function analysis of the bestrophin family of anion channels." *J Biol Chem.* (2003); 278(42): 41114-25.

Tsutsumi S., Kamata N., Vokes T.J., Maruoka Y., Nakakuki K. "The novel gene encoding a putative transmembrane protein is mutated in gnathodiaphyseal dysplasia (GDD) ." *Am. J. Hum. Genet* (2004); 74(6): 1255–1261.

Ukhanov K, Leinders-Zufall T & Zufall F. "Patch-Clamp Analysis of Gene-Targeted Vomeronasal Neurons Expressing a Defined V1r or V2r Receptor: Ionic Mechanisms Underlying Persistent Firing." *J Neurophysiol* (2007); 98(4): 2357-2369.

Vassar R., Ngai J., Axel R. "Spatial segregation of odorant receptor expression in the mammalian olfactory epithelium." *Cell* (1993); 74(2): 309–18.

Vermeer S, Hoischen A, Meijer RP, Gilissen C, Neveling K, Wieskamp N, de Brouwer A, Koenig M, Anheim M, Assoum M, Drouot N, Todorovic S, Milic-Rasic V, Lochmüller H, Stevanin G, Goizet C, David A, Durr A, Brice A, Kremer B, van de Warrenburg BP, Schijvena. "Targeted next-generation sequencing of a 12.5 Mb homozygous region reveals ANO10 mutations in patients with autosomal-recessive cerebellar ataxia." *Am J Hum Genet.* (2010); 87(6): 813-9.

von Campenhausen H., Mori K. "Convergence of segregated pheromonal pathways from the accessory olfactory bulb to the cortex in the mouse." *Eur. J. Neurosci* (2000); 12(1): 33–46.

Wagner S, Gresser A.L., Torello A.T., Dulac C. " A multireceptor genetic approach uncovers an ordered integration of VNO sensory inputs in the accessory olfactory bulb." *Neuron* (2006); 50(5): 697–709.

Wang RT & Halpern NM. "Neurogenesis in the vomeronasal epithelium of adult garter snakes. III. Use of 3H-hymidinebipolar neurons. ." *Am. J. Anat.* (1988): 178–185.

Wang RT & Halpern NM. "Neurogenesis in the vomeronasal epithelium of adult garter snakes. I. Degeneration of bipolar neurons and proliferation of undifferentiated cells following experimental vomeronasal axotomy." *Brain Res* (1982a): 23–39.

Wang RT. & Halpern NM. "Light and electron microscopic observations on the normal structure of the vomeronasal organ of garter snakes." *J. Morph* (1980); 164(1): 47–67.

Wendy E. Grus, Peng Shi , Ya-ping Zhang and Jianzhi Zhang. "Dramatic variation of the vomeronasal pheromone receptor gene repertoire among five orders of placental and marsupial mammals." *PNAS* (2005); 102(16): 5767-5772.

Wilson, E. O. "Chemical communication within animal species." *Chemical Ecology* (1970): 133–155.

Wilson, KC. & Raisman G. "Age-related changes in the neurosensory epithelium of the mouse vomeronasal organ: extended period of postnatal growth in size and evidence for rapid cell turnover in the adult." *Brain Res.* (1980); 185(1): 103–113.

Wu Y, Tirindelli R, Ryba NJ. " Evidence for different chemosensory signal transduction pathways in olfactory and vomeronasal neurons." *Biochem Biophys Res Commun* (1996); 220(7): 900–904.

Wyatt TD. *Pheromones and Animal Behaviour*. Cambridge: Cambridge University Press, 2003.

Yang H, Kim A, David T, Palmer D, Jin T, Tien J, Huang F, Cheng T, Coughlin SR, Jan YN, Jan LY. "TMEM16F forms a Ca2+-activated cation channel required for lipid scrambling in platelets during blood coagulation." *Cell.* (2012); 151(11): 111-22.

Yang YD, Cho H, Koo JY, Tak MH, Cho Y, Shim WS, Park SP, Lee J, Lee B, Kim BM, Raouf R, Shin YK, Oh U. "TMEM16A confers receptor-activated calcium-dependent chloride conductance." *Nature* (2008); 455(7217): 1210–1215.

Yang C & Delay RJ. "Calcium-activated chloride current amplifies the response to urine in mouse vomeronasal sensory neurons." *J. Gen. Physiol* (2010); 135(1): 3–13.

Ye RD., Boulay, F., Wang, JM., Dahlgren, C., Gerard, C.,Parmentier, M., Serhan, C.N., and Murphy, P.M. "International union of basic and clinical pharmacology. LXXIII Nomenclature for the formyl peptide receptor (FPR) family." *Pharmacol. Rev* (2009); 61(2): 119−161.

Yu K, Duran C, Qu Z, Cui YY, Hartzell HC. "Explaining calcium-dependent gating of anoctamin-1 chloride channels requires a revised topology." *Circ Res* (2012); 110(7): 990-9.

Yu K, Lujan R, Marmorstein A, Gabriel S, Hartzell HC. "Bestrophin-2 mediates bicarbonate transport by goblet cells in mouse colon." *J Clin Invest.* (2010), 120(5): 1722-35.

Yu TT, McIntyre JC, Bose SC, Hardin D, Owen MC, McClintock TS. "Differentially expressed transcripts from phenotypically identified olfactory sensory neurons." *J Comp Neurol* (2005); 483(3): 251-62.

Zhang P, Yang C, Delay RJ. "Urine stimulation activates BK channels in mouse vomeronasal neurons." *J Neurophysiol* (2008); 100(4): 1824–1834.

Acknowledgement

Carrying out my PhD work has been perhaps the most challenging activity of my life. I have shared the best and worst moments of my doctoral journey with many people. It has been a great privilege to spend several years in the International School of advance Studies.

My first debt of gratitude must go to my advisor, Prof. Anna Menini. She patiently provided the vision, encouragement and advice necessary for me to proceed through the doctoral program and complete my dissertation.

I am extremely thankful to Dr. Simone Pifferi for his valuable guidance in experiment and in the thesis. To my lab mates and SISSA staff who also deserve my sincerest thanks, their cooperation and assistance has meant more to me than I could ever express.

To my lovely friends, Vikas, Swathi, Priya, Zainab and Nadeem Sb who supported me in the past four years. They were on my side in the gloomiest phase.

Thanks to my husband, with whom I started enjoying my life. You already have my heart. “Bande” I can just say thank you for your love and encouragement, which allowed me to finish this journey. I also want to thank to my in-laws for their unconditional support. Amma and Shazia thank you so much.

And finally, I would like to thank Ayesha, Ume and Bhai and my parents to whom I am dedicating this thesis. Ami daddy I owe you everything and just wish I can show you how much I love you.

Asma Amjad

Trieste 28-09-2013